Atmospheric Sciences Research center

5118551 4

80325

NAG1-583

P. 64

Final Report NASA Grant NAG-1-583

Measurement of heat and moisture fluxes at the top of the rain forest during ABLE

Principal Investigator: David R. Fitzjarrald

We have now completed work planned for the duration of this grant. We have submitted a paper based on our work to the <u>Journal of Geophysical Research</u>. The bulk of this report consists of this paper (Appendix A). In addition, one student, Brian L. Stormwind has completed his degree requirements for the M. S. in Atmospheric Sciences based on data obtained during this experiment, of which he was a participant, and with financial support of this grant. We include the abstract of his thesis here as Appendix B. Many of the difficulties we encountered during the ABLE-2a mission led to data acquisition improvements during our participation in ABLE-2b, whose field phase was completed in May 1987.

David R. Fitzjarrald
July 10, 1987

(NASA-CR-181076) MEASUREMENT OF HEAT AND MOISTURE FLUXES AT THE TOP OF THE RAIN FOREST DURING ABLE Final Report (State Univ. of New York) 64 p Avail: NTIS HC A04/MF A01 CSCL 02F G3/43

N87-27307

Unclas 0080325

APPENDIX A

Turbulent transport observed just above the Amazon forest

David R. Fitzjarrald

Brian L. Stormwind

Atmospheric Sciences Research Center
State University of New York, Albany

Gilberto Fisch*
Instituto Nacional de Pesquisas da Amazônia
Manaus, Amazonas, Brazil

Osvaldo M. R. Cabral
Centro Nacional de Pesquisa da Serigueira e Dende
EMBRAPA
Manaus, Amazonas, Brazil

*Current affiliation: Centro Técnico Aeroespacial, Instituto de Atividades Espaciais, Divisão de Ciências Atmosféricas, São José dos Campos, S. P., Brazil

ABSTRACT

We present observations of turbulent heat, moisture, and momentum transport made at two levels, approximately 5 and 10 m above the Amazon rain forest canopy. Data acquired at 10 Hz included variances and some mixed third moments of vertical velocity, temperature, and humidity. Two features of the data appear to question the displacement height hypothesis: 1) The characteristic dissipation length scale in the near-canopy layer varied between 20 m in stable conditions to approximately 150 m during afternoon convective conditions, generally larger scales than would be expected; and 2) No appreciable difference in dissipation scales was seen at the two observed levels. Observed peaks in vertical velocity-temperature cospectra lead to similar length scale estimates for dominant eddies. Heat budgets on selected days show that frequent periods with negative heat flux concurrent with continuing positive moisture flux occur in early afternoon, and this is believed to indicate the patchy nature of canopy-atmosphere coupling. Vertical velocity skewness was observed to be negative on three successive days and exhibited a sharp positive gradient. We present time series of some of the terms in the turbulence budgets46 of vertical velocity variance and kinematic heat flux.

1. Introduction

Because of its extent, the Amazon rain forest is believed to play an important role in the global budgets not only of heat and moisture, but also of ozone, CO, CO_2, natural hydrocarbons, and other compounds [Harriss *et al.*, 1987]. Understanding turbulent exchange processes that couple the forest with the atmosphere is a necessary step in performing budget analyses anywhere, but it has additional significance in regions in which direct measurements are and will continue to be rare, such as the tropical rain forest. Direct measurement of fluxes of many trace gases, for example, is not currently feasible. Fluxes are frequently estimated using flux-gradient relations originally developed for flow over smooth, flat surfaces. The description of exchange of non-reactive substances over such surfaces is well described using similarity hypotheses [Wyngaard, 1973]. Because of the geometric complexity of forest canopies, several different characteristic length scales could be important, and this fact makes similarity analysis questionable. At the same time, the practical need for simple parametric methods to determine fluxes impells one to seek the limits to which the known results suffice. It thus seems reasonable to ask in what ways does turbulent exchange above forest canopies differ from that which occurs above the plane surface.

Theoretical and practical needs for better understanding of turbulent exchange processes between the atmosphere and tropical forests led us to measure turbulent transport of moisture, heat, and momentum above the tropical rain forest in the Amazon. Our second motivation was to measure the surface buoyancy flux in support of a parallel study of the convective boundary layer growth. Work on this subject will appear in a companion article [Martin *et al.*, 1987]. In Section 2 we discuss the observation site and the types of instruments used. Correct interpretation of turbulence properties frequently depends critically on the manner in which data were acquired and processed, and how the instruments were exposed, topics discussed in Section 3. Characteristic length scales are discussed in Section 4. In Section 5 we consider heat and moisture budgets along with average diurnal properties of the near-canopy layer. Case studies illustrate changes in turbulent transport seen after rainfall and properties of nocturnal turbulence. We

examine observed properties of the vertical velocity skewness and of some components of the turbulent budget of vertical velocity variance in Section 6 and present conclusions along with plans for future work in Section 7.

2. Experimental site and instrumentation.

Data presented in this paper were taken at the Ducke Forest Reserve (2° 57' S, 59° 57' W) during July and August 1985 on a 45 m tall scaffolding tower as part of the ABLE-2a experiment. This tower, currently the only platform available for performing turbulence measurements in the Amazon rain forest, was erected in 1983 by members of the Anglo-Brazilian micrometeorological program. Details of the surrounding vegetation and a photograph of the tower are given in Shuttleworth *et al.* [1984, here referred to as S84]. The canopy reaches approximately to 35 m height, with occasional isolated trees reaching up to 40 m. In most directions, there is undisturbed forest surrounding the site for several kilometers. The forest is somewhat disturbed west of the tower, but the predominant wind direction in this season is easterly, minimizing this problem.

Where possible, we take advantage of supporting measurements being done at the Ducke tower. This instrumentation, described in S84, includes anemometers and thermometers at various tower levels. At the 45 m level two Didcot Industries automatic weather stations (AWS, described in S84) provided measurements of net and incoming solar radiation, humidity, and temperature. The Hydra, a device that measures eddy fluxes of heat, moisture, and momentum developed by the Institute of Hydrology in the UK [S84], operated at 48.5 m. In this paper, we take the degree of agreement of flux observations between the Hydra and our instrumentation as one measure of data quality. Because the profile data system was undergoing tests during the time when we operated, we have turbulent moment information without support of the more traditional gradients. This limits our ability to estimate stability indices and prevents direct estimation of various production terms in turbulence budgets but still allows a general description of turbulence properties.

We brought additional rapid-response instruments to measure temperature, humidity, and vertical velocity at 39 and 45 m height, just

above the approximate canopy top of 35 m. At the upper level we installed a standard Gill propeller-vane anemometer. The rapid-response instruments, all manufactured by Campbell Scientific Inc., included two single-axis sonic anemometers, each with a fine-wire thermocouple, and two krypton hygrometers. Tanner *et al.* [1985] and Campbell and Tanner [1985] describe these instruments in more detail. The krypton hygrometer operates on the same principle of absorption of ultraviolet light by water vapor as does the more familiar Lyman-α hygrometer [Buck, 1976]. The principal advantages of the krypton device are low operating power and long source tube life. It exhibits somewhat lower sensitivity than does the Lyman-α device, but previous tests [Campbell and Tanner, 1985] indicate that performance is adequate, especially in the high-humidity environment of the Amazon. The hygrometer operated on battery power when the main data system (described below) was disconnected. The primary difficulty we found with our hygrometers was a tendency for the signal strength to decrease with time. Cleaning the windows periodically restored the signal to its original strength.

It is difficult to operate this type of instrumentation in the tropical rain forest. We often had to replace the fine-wire thermocouples as they were broken by raindrops, and in one case the thermocouple was incorporated overnight into a spider web. Heavy rain also damaged the anemometer transducers, though the anemometers functioned properly after light rain (see Section 5). We note that these instruments are capable only of measuring fluctuations, not mean values, of the three parameters w, T, and q. We have used the manufacturers' calibrations throughout.

At each level, an instrument set, consisting of an anemometer and thermocouple assembly with the hygrometer $\approx$ 0.3 m distant mounted on a small transverse bar, was placed at the end of a guyed boom extending 3 m from the tower. The top boom faced east and the bottom one faced south. To minimize interference of the horiziontal wind with the vertical wind measurement, we levelled each anemometer vertically by adjusting the guy wires, observing the image of bubble levels through a right-angle prism with a telescope. It is difficult to assess to what precision we obtained level initially or how that level was maintained with time. We believe that the anemometers were level initially to within 0.3°. The instruments were serviced and levelled at least once a

day, and usually more frequently. We are aware that the local vertical may not necessarily be perpendicular to the local streamline. However, since we operated only single-axis sonic anemometers, we felt that using the local vertical to orient each instrument was a valid compromise.

We operated two separate data acquisition systems and three data archiving systems in parallel. The main system consisted of a PDP 11/73 computer and floppy disk unit. We constructed a data acquisition program for our computer incorporating many of the features of the program in use at the Boulder Atmospheric Observatory (Kaimal and Gaynor, 1983). Our aim was to calculate as many derived quantities as possible in real time. Since we had very limited data storage capability, no raw data were saved. Data were acquired at 10 Hz, and means, standard deviations, higher moment quantities, certain block-averaged spectra and cospectra, and ten-second averaged data (see Table 1) were obtained and archived for twenty-minute periods. Block averaging of spectra and cospectra was done in the manner described by Kaimal and Gaynor (1983). All moment quantities were accumulated over the twenty-minute period. Ten sets of 2-minute spectra and cospectra are included in the averages saved at the end of each twenty-minute period. Two errors in the data acquisition program caused us to lose some information. First, the ten-second averaged data has thirty seconds of missing data each two minutes. This has no effect on fluxes or estimates of the high-frequency end of the spectra and cospectra, calculated in real time, but it means that we cannot use the ten-second average data to make low-frequency spectral estimates. Second, a scale factor was missing for the cospectral and quadrature spectral calculations. This prevents us from estimating the coherence or spectral correlation coefficient but does not affect cospectral shapes.

In parallel, variances, fluxes, and some covariances (see Table 1) were calculated with a Campbell Scientific Datalogger. Grab samples were taken at approximately two-second intervals with this system. These data were recorded both by a small cassette tape and by a Commodore microcomputer. All equipment were powered by a small gasoline-powered electric generator. During periods when the generator was disconnected and the site was unattended, the instruments operated on battery power, with data processed by the Datalogger and recorded only by the cassette recorder.

At the end of the experiment we fitted the inertial subrange portion of the power spectra with a least-squares line of slope -5/3 to determine the dissipation rate ϵ of turbulent kinetic energy and the estimates of the rate of destruction of temperature and specific humidity variance, as detailed in Panofsky and Dutton [1983]. The fits were quite good (Fig. 1a), and this gives us confidence in the high-frequency response of the instruments. We did not observe significant power in the wT and wq cospectra above 0.5 Hz (Fig. 1b). It appears that fluxes can be obtained with instruments with a sampling interval of two seconds. Peaks in the cospectra present in Fig. 1b occur at too low a frequency to be considered significant; we will estimate characteristic length scales from cospectral data using data from a subsequent experiment in a subsequent publication. We return to the discussion minimum sampling interval requirements in Section 3.

It proved essential that there was redundancy in the data processing and recording systems. Some periods when the cassette recorder was turned off accidentally were covered by data recorded on the microcomputer. Until the first week of August, the computers operated at ambient temperature and humidity at the forest floor. As a result, mold growing in the PDP disk drive caused that system to fail on 1 August. Thus, this study focusses on turbulence budgets and higher moments during the last week in July when the main data system worked, and deals more with fluxes, covariances, and the heat budget during the first week in August.

3. Instrument and data acquisition system intercomparisons

In this section we discuss errors commonly associated with the eddy correlation method and assess the quality of our measurements. We operated single-axis sonic anemometers to measure vertical velocity fluctuations, the simplest observational equipment adequate for doing eddy correlation measurements. We compare results obtained using different instruments and/or data analysis techniques and take agreement among the systems to be a valid empirical measure of reliability of our measurements. A daunting number of possible sources of error in making eddy correlation flux estimates have been identified. These include introduction of the horizontal velocity component into the vertical measurement because of inappropriate sensor alignment, usually

overcome during operation of three-component anemometers by rotating the coordinate system to minimize the w component [Wesely, 1970]. In the case of the Reynolds stress this problem is particularly serious. McMillen [1986] notes that errors estimated by a number of researchers range from 8% to 100% per degree of misalignment. He shows sample data in which the unrotated estimates of the momentum flux were positive, with more plausible negative results obtained with rotations. There is also the problem of flow around the obstacle of the tower itself [Wieringa, 1980], believed to affect surface-layer flux measurements. Path-length averaging over the distance between the sonic anemometer transducers (here, 20 cm) can add from 5 to 10% error to estimates of heat and moisture fluxes and is believed to lead to even greater errors for estimates of the momentum flux [Moore, 1986]. This error depends on the size of eddies carrying the flux and may not be a serious factor here. Interference due to flow around the framework of the sensor itself may result in errors in scalar flux measurements done with sonic anemometers that canl reach 25% [Wyngaard, 1981] . To make matters worse, the eddy correlation flux itself is a statistical quantity. Each flux estimate can be viewed as a sample from an ensemble of measurements. We expect run-to-run variability in a surface layer of at least 10% in ideal conditions [Wesely and Hart, 1985], with the amount varying according to the dominant scale of the turbulence and the variance of the measured variable [Lenschow and Kristensen, 1985].

Faced with such an imposing array of possible objections to the validity of our measurements, we would have been terminally discouraged from attempting the analyses presented here were it not for the results of a series of intercomparisons between different instruments and data processing systems. Before the experiment, we compared the two sensor systems in a disturbed surface layer, finding a 5% average difference in σ_w, and this difference magnified disagreements in higher moments to 30%. Since our instruments faced in different directions on the tower, we assess the importance of the obstacle effect of the tower on the measurements by comparing heat flux measurements according to the quadrant of the prevailing wind. The results (Fig. 2) do not show any identifiable difference in flux when one or the other instrument is poorly exposed. To address the problem of the inherent variability of the eddy flux related to uncertainties in the ensemble

average, we compare fluxes at the top level calculated using the Micrologger and the PDP system, respectively. On 25 July (Fig. 3a) the 20 minute averaging period for each system began on the same minute, and the fluxes agree quite well. Recall that we compare samples taken at 10 Hz by the PDP system with grab samples each 2 seconds by the Datalogger. On 26 July (Fig. 3b), the data averaging periods were 10 minutes displaced, and one sees that there is variability of ≈20-30% at times in the twenty-minute averages, though the cumulative transport was calculated to converge and hourly averages agreed quite well. Finally, we compare our measured heat flux with that obtained by the independent Hydra system (Fig. 3b, marked by H), and see good agreement. We do not think that the various types of error lead to very large (> 20%) absolute errors in our data. Comparison of fluxes measured at the two levels (see below) is good, and this indicates that the relative error between the two instrument packages was smaller. This is probably because the daytime heat flux is accomplished by rather large convective eddies (see below). Since we were interested only in q fluctuations, we calculated only the percentage deviation of the hygrometer signal from its mean [e.g., Tanner *et al.*, 1985]. The mean used was the two-minute average just prior to observations for the PDP system. This mean was a two-minute running mean for the Datalogger system. Differences in the estimated moisture flux derived from the same signals as large as 20% between the systems were observed. This may have occurred because of the difference in the definition of the mean hygrometer output from which the deviation quantity was calculated. When data from the two levels are compared, only data from one acquisition system are used.

We have estimated the covariance uw directly using w from the top sonic anemometer and u from the Gill propeller vane. These instruments were at 45 m height, separated by about 4 m. Hicks [1972] showed the frequency limits to which propeller anemometers may be used in eddy correlation measurements. We expect acceptable results if the bulk of the momentum flux is contained in frequencies lower than a cutoff frequency determined by the Gill response characteristic. This appears to have been the case during this experiment, as is demonstrated by noting that the frequency above which the uw cospectral values are near zero occurs at much lower frequency than the frequency at which the Gill anemometer loses sensitivity, departing from the inertial subrange

prediction (Fig. 1b). The second and third techniques are simply to associate u_* with the vertical velocity standard deviation σ_w at each level, relying on the surface-layer analogy [Panofsky and Dutton, 1984, p. 161]: $\sigma_w = 1.25\, u_*\, F[(z-d)]/L$, where F is an empirical function and L is the Monin-Obukhov length. Since the function F is not strongly dependent on (z-d)/L (a one-third power law that comes from matching the free convection similarity prediction), and since we observe the daytime range of (z-d)/L at Ducke to be confined to the range 0. to -0.5, we take the stability effect to be constant and hypothesize simply that $u_* \approx \sigma_w/1.25$. Results of the intercomparison of this indirect estimate with the direct calculation $\sqrt{(-uw)}$ were surprisingly good. Furthermore, these estimates are in good agreement with u_* obtained by the independent Hydra system (Fig.4). Busch [1973] despaired of estimating u_* from σ_w in the surface layer to better than 50%, but this appears to be overly pessimistic in this case. In S84 and Moore [1986], the authors cautioned that the Hydra u_* estimates could not be trusted to within a factor of two. In our opinion, it is unlikely that these three nearly independent estimates of u_* would agree to within 20% if errors as large as the most pessimistic estimates were present. We are not suggesting that the sources of error discussed by the various authors above are not real. Rather, it is possible that the scale of the flux-containing eddies for our particular case is so large that the eddies can be resolved with our crude instrumentation.

4. Characteristic length scales just above the canopy

We search for the limits of applicability of plane surface layer similarity theory to the layer just above the forest canopy by asking a simple basic question: What is the characteristic turbulent length scale in this layer? It is customary above forest canopies to associate the characteristic turbulent length scale with the height above an assumed displacement height d, above which features of the plane surface layer are supposed to obtain. The displacement height is frequently estimated by attempting to identify logarthmic wind profiles just above canopy or (more commonly) taken to be some fraction of the mean canopy height [Jarvis, *et al.*, 1976].

One way to check the validity of the displacement height hypothesis is to identify the characteristic turbulent length scale with

the dissipation length scale ℓ for turbulence in the region just above the canopy:

$$\epsilon = u_*^3/\kappa \ell \quad , \qquad (1)$$

where ϵ is the dissipation rate obtained from the slope of the w power spectra in the inertial subrange and κ is the von Karman constant. Recall that ℓ is simply the height above the ground in the case of the plane surface layer. If the layer just above canopy top were similar to a plane surface layer displaced up d meters in all respects, we would expect to find $\ell \approx \kappa(z - d)$ to be a characteristic length in neutral conditions, increasing with increasing $(z-d)/L$. We would expect to see a different characteristic scale at each of the two levels, and that this scale would be approximately 5 - 10 m, according to the estimates of d above. Our results (Fig. 5a,b, using two different estimates of u_*) show that the characteristic scales are much larger than this, but they do show the expected decrease as the layer became less convective. A similar plot obtained using $u_*=\sigma_w/1.25$ at the 39 m level (because we do not have direct estimates of uw at this level) did not show any significant difference. Wyngaard [1982] noted that largest eddies feel the strongest buoyancy effects, and we see that conditions only need to be slightly convective for the dissipation length scale to increase greatly. We did not plot this scale length versus $(z-d)/L$ because we are not certain that z-d is the appropriate length scale.

5. Diurnal cycles

Mean temperature and humidity time series at the top of the tower (Fig. 6a,b) illustrate the rapid morning temperature rise and the nearly constant specific humidity. The small bulge in specific humidity appearing in the mean at approximately 0900 LST is believed to be related to the morning convergence of turbulent moisture flux into the boundary layer. The vapor is temporarily trapped in a shallow boundary layer that persists until the remains of the nocturnal stable layer are eroded by the surface heat flux [Martin, *et al.*, 1987]. The temperature and humidity standard deviations (Fig. 7a) throughout the day are nearly the same at the two levels, but the vertical velocity standard deviation at the top level is appreciably larger than that at the bottom level. It is frequently assumed that heat and moisture or other scalars are

transported in a similar manner. While the diurnal course of the w-T correlation coefficient (Fig. 7b) runs from +0.5 to -0.4, similar to that seen in the surface layer during the Kansas experiments [Haugen *et al*, 1971], we note that the w-q correlation coefficient is always positive and does not exceed approximately 0.3. Moreover, the T-q correlation coefficient never exceeds 0.5. The low T-q correlation could be explained simply by presence of high frequency noise in the q signal, but power spectra do not show this to have been a problem during the daytime. The precipitous drop in the hourly-averaged T-q correlation near noon is a reflection of reduced heat fluxes seen at that time on several of the days included in the average (Fig. 8). We observed rain showers at or near the tower on these days. Water on the leaves led to transient stable periods in the canopy layer (see below).

The heat budget for the canopy can be written approximately as:

$$R_n = LE + H + G + S \,, \qquad (2)$$

where R_n is the net radiation, LE the latent heat flux, H the sensible heat flux, G the heat storage within the canopy (both in the air and in the biomass) and S the heat flux from the soil. The plot of the mean heat budget (Fig. 7c) is similar to those presented in S84, but the residual ($LE + H - R_n$) is larger.

We see that the layer just above the Amazon forest can be confirmed to be a constant flux layer. This feature of the smooth plane surface layer obtains. We cannot easily explain the large residual term seen in the heat and moisture fluxes. In S84 the authors note that there is very little solar radiation that penetrates to the forest floor in the Amazon, and we can probably ignore the soil heat flux term. We estimated the heat storage in the canopy air on selected days and found that it did not exceed 20 W/m^2. Fisch [1986] estimated the biomass heat storage from measurements of temperature changes within trees at the Ducke site using data from previous field experiments. He found that midday maxima of biomass heat storage to be in the range of 60-80 W/m^2. It is puzzling that our heat budget does not balance as well as it does for previous experiments at the same site. Since intercomparison with the Hydra measurements of the latent and sensible heat fluxes was good, we

would obtain a similar residual with that system. S84 report scatter in the hourly values of two automatic weather station net radiation estimates of 10 to 15%, and perhaps the imbalance in the average heat budgets can be ascribed at least partially to this measurements. We note that Verma *et al.* [1986] had similar difficulty in achieving heat budget balance to better than 30%, but their residual was not consistently of the same sign.

What the averages do not show is the large day-to-day variability. One of the surprising features of the Amazon surface layer is that one frequently observes very small or negative heat fluxes in the early afternoon. (See Fig. 8, 26 July, and 1,2,3, and 5 August). They are all associated with reduced incoming solar radiation, as clouds built up. It was common to see isolated storms in the early afternoon during the first week in August. We observed cool, relatively dry gusts to pass over the tower during this time of day and presume them to have been the result of downdrafts penetrating from convective clouds. Note that the latent heat flux remained high on most of these days even as the heat flux (and frequently also the virtual heat flux) vanished. The surface layer can be thrust for a time into a curious daytime state in which mixing must be accomplished by mechanical eddies. It is clear that horizontal advection must also play a role in balancing the heat budget at this time.

Water deposited on leaves and returned immediately to the atmosphere during transient episodes represents moisture transfer not properly understood by surface resistance models, in which stomatal control is important [Shuttleworth and Calder, 1979]. Between 1200 and 1215 on 24 July, we observed a light shower at the Ducke tower. Rainfall amounts were not large enough to be registered by the recording raingauge at the top of the tower, but there was a remarkable disruption of the diurnal heat budget (Fig. 9a). Note the drastic reduction in heat and moisture fluxes just after the shower, followed by a huge latent heat flux at 1300 LST. Two independent measurements of this latent heat flux show it to exceed even the measured incoming solar radiative flux. We surmise that during this time there must be appreciable sensible heat flux advection from nearby areas which the rain shaft did not cross. With cooling of the canopy surface layer, there was lowered momentum flux, as indicated by the drop in the drag coefficient at midday on 24 July (Fig. 9b). Time series of ten-second average data between 1221 and 1321 (Fig. 9c-d)

illustrate the stages of the recovery. During the first twenty minutes variation in w, q, and T was suppressed. Then wide excursions in q and T with little vertical motion occurred during the second twenty minutes. These we suppose to correspond to the time when weak plumes can rise from the forest, recondense and become visible. Finally, after 1300, vigorous vertical motion returned and the water on the leaves was returned to the atmosphere. These small rain showers were seen frequently from the top of the tower. Often we observed fog forming in low-lying areas in the wake of the passing showers similar to this case. Later, plumes rose from the forest, and on some occasions new convective clouds formed. We see that a limited, decoupled area with a very low drag coefficient was created in the middle of the forest. We suggest that these "wet, slick spots" may provide a convergent location downwind for preferential development of new convection, providing that the sky clears again and the storm does not occur too late in the day.

It might be argued that the tropical oceans and the tropical rain forests perform similar roles in providing latent heat to large scales of atmospheric motions. The maximum latent heat fluxes reported here ($\approx$ 650 W/m^2) are much larger that those reported over the tropical ocean ($\approx$ 100 W/m^2, undisturbed conditions and $\approx$ 200 W/m^2 during disturbed conditions during GATE, Barnes [1980]). Maximum sensible heat fluxes are five to ten times larger than those seen over the tropical ocean, but the total daily transport of moisture is comparable in each case, as the oceanic fluxes occur all day. The large diurnal amplitude of the sensible heat and latent heat fluxes are known to lead to much deeper rapid cloud formation, with transient effects penetrating to higher latitudes [Silva Dias *et al.*, 1983]. Hence, the tropical rain forest is very much a continental environment, not at all a "continental ocean".

6. Higher turbulent moments

We found the skewness of the vertical velocity, Sk(w), to be negative, decreasing sharply from the 39 m level to the 45 m level (Fig. 10). Our observed negative vertical velocity skewness and steep vertical gradient is in accord with previous studies of turbulence above model plant canopies [Raupach and Thom, 1981], but contrasts with positive skewness seen in the convective plane surface layer [Chiba, 1978]. Raupach and Thom [1981] and Denmead and Bradley [1985] relate negative negative

vertical velocity skewness to the presence of gusts that intermittently penetrate deep into the canopy. Raupach and Thom show that the skewness of the vertical velocity, Sk(w), decreases rapidly with distance above obstacles of height h in the wind tunnel. The wind-tunnel results show Sk(w) of -0.4 and -0.2, at $z/h \approx 1.2$ and 2., respectively, where h is the obstacle height. If we take h to be the mean canopy height, we observe similar values of skewness (Fig. 2) over the Amazon during the day, at $z/h \approx 1.1$ and 1.3. Raupach and Thom note that $Sk(w) < 0.2$ may be a condition for inertial sublayer flux-gradient relations to hold.

We use data from the two instrumented levels to form the turbulent balance of σ_w^2 on 24-26 July, 1985. We are aware of the large errors that can arise not only in estimating third moment quantities and but also from differencing two such estimates. However, the reasonable results obtained from the skewness study indicates that the signal may be large enought to detect, and we intend only to look for qualitative features of these budgets. For simplicity, we consider the horizontally homogeneous situation, and the relevant budget equations are [Businger, 1982]:

$$(1/2)\,\partial\sigma_w^2/\partial t = \underset{b}{(g/\Theta_0)\,\overline{wT}} - \underset{t}{(1/2)\,\partial\overline{w^3}/\partial z} - \underset{p}{(1/\rho_0)\,\overline{w\,\partial p/\partial z}} - \underset{d}{\epsilon/3} \quad (3)$$

Mean and eddy terms are given by upper- and lower-case symbols, respectively. Symbols t, p, b, and d denote terms of turbulent transport, pressure gradient covariance transport, buoyant production, and dissipation, respectively. Any residual found with in the budget analysis includes unmeasured terms as well as the sum of errors. In a conventional surface layer, Wyngaard [1973] noted that increased buoyant production is offset by increased transport as the layer becomes more convective. Our budget results (Fig. 11) show there to be consistent anticorrelation between these terms. The local time change terms (not plotted) were negligible. Note that a near balance of the buoyant production and transport terms would occur in a normal surface layer for convective conditions, $z/-L > 1$ or so. Assuming $d \approx 26$ m, we find typical daytime values of $(z-d)/-L \approx 0.5$ over the forest at Ducke, somewhat less convective conditions. Our measurements indicate that local dissipation

does not play as dominant a role in the near-canopy layer as has been observed in plane surface layers.

Transport terms are known to be important in second-moment budgets above vegetation [Raupach, 1987]. The horizontally homogeneous heat flux budget is [Businger, 1982]:

$$\underset{}{\partial \overline{w\theta}/\partial t} = \underbrace{(g/\Theta_0)\,\sigma_\theta^2}_{b} - \underbrace{\partial\,\overline{w^2\theta}\,/\partial z}_{t} - \underbrace{\overline{\theta\,\partial p/\partial z}}_{p} - \underbrace{\sigma_w^2\,\partial\Theta/\partial z}_{G} \qquad (2)$$

Symbols are as in (1) and G represents the gradient production term. We estimated the heat flux budget using hourly averages of the moments $\overline{w^2\theta}$ at 39 m and 45 m to calculate the transport terms. Though we do not have direct measurements of the temperature gradient, we estimated the gradient production term G using the observed range of σ_w with characteristic afternoon temperature gradients measured at Ducke tower during an earlier experiment [Shuttleworth *et al.,* 1985]. The results on two days (Fig. 11) indicate that the buoyant production term over the Amazon, comparable in magnitude to the transport term, cannot be ignored. During periods of transient daytime stabilization, buoyant production may by a dominant term in this balance. For example, at approximately 1300 LST on 26 July, we observed the heat flux to become negative and presumably the temperature gradient inverted. We estimated the gradient term in this case using the observed σ_w and the temperature gradient report from the earlier experiment just after an afternoon rain shower (marked G' on the figure). Although the result can hardly be considered conclusive, it indicates that is is plausible that the gradient term and the buoyant production terms made the budget balance during this period. These preliminary budget analyses emphasize the importance of transport and buoyant production terms in the flux budget. Future work is needed to quantify these terms, in particular as part of an assessment of the validity of flux-gradient relations in the near-canopy layer.

7. Conclusions and future plans

Three general conclusions may be made: First, the length scale of turbulence just above the Amazon forest is large enough, and the correlations between vertical velocity fluctuations and other parameters

strong enough that heat, moisture, and momentum fluxes can probably be estimated to within 20% with single-axis sonic anemometers, despite the many possibilities for error. Moreover, sampling at 0.5 Hz probably is sufficient to measure daytime eddy fluxes of heat and moisture. Second, the displacement height analogy between the smooth plane surface layer and the layer just above a forest canopy is limited. We found the dissipation length scale not to increase with height just above the forest and confirmed that the skewness of the vertical velocity is negative, both exceptions to the plane surface layer similarity hypotheses. Third, there is considerable patchiness to transports above the rain forest due to the occurrence of intermittent stabilization associated with convective storm outflows and rainwater deposited on leaves. Parameterizations of the coupling between the rain forest canopy and the atmosphere based primarily on data obtained on undisturbed days (when instruments tend to be operating) may estimate total transports of heat and moisture poorly.

It is clear that future work should be done not only to confirm results here for the near-canopy layer, but the mechanism of gust penetration into the canopy itself must also be understood. We have conducted a further field experiment to study these mechanisms, instrumenting more levels between the canopy top and the surface in the Amazon, and this will be reported in due course. We note in conclusion that it may be more practical to measure turbulent fluxes directly or to use parameterizations that require measurements only at a single level, such as one based on temperature skewness [Tillman, 1972], than to search for "universal" flux-gradient relations in the near-canopy layer.

8. Acknowledgements

This work, part of the NASA ABLE-2a experiment, was supported by grant NAG-1583 from that institution. John W. Sicker at the Atmospheric Sciences Research Center (ASRC) provided expert technical support with the electronics and instrumentation. G. G. Lala, also of ASRC, helped with the PDP data acquisition program. Jorge L. M. N. Noqueira of the National Institute for Space Research (INPE) in Brazil helped with emergency field repairs on a sonic anemometer that made section 5 of this work possible.

We clearly owe a great debt to J. Shuttleworth and his associates at the Institute of Hydrology (IH) in the United Kingdom and

their Brazilian collaborators, among them Luis Molion and colleagues at INPE as well as Ari De O. Marques Filho and associates at the National Institute for Amazon Studies (INPA) in Manaus. It was through the efforts of the Anglo-Brazilian micrometeorological program that the tower was constructed and instrumented at the Ducke site. We thank researchers from IH, C. J. Moore among others, for useful discussions and for providing data used for intercomparisons in this work. D. Baldocchi, M. Wesely, D. Lenschow, and anonymous reviewers made suggestions that greatly improved the manuscript.

REFERENCES

Barnes, G., Subcloud Layer Energetics of Precipitating Convection. Ph.D. dissertation, University of Virginia, Charlottesville, VA, 180 pp., 1980.

Buck, A.L., `The Variable-Path Lyman-alpha Hygrometer and its Operating Characteristics', Bull. Am. Meteor. Soc., Vol. 57, No. 9, 1113-1118, 1976.

Busch, N.E., `On the Mechanics of Atmospheric Turbulence', in Haugen, D.A. (ed.), Workshop on Micrometeorology, Am. Meteorol. Soc., 1-65, 1973.

Businger, J.A., `Equations and Concepts', in Nieuwstadt, F.T.M. and VanDop, H. (eds.), Atmospheric Turbulence and Air Pollution Modelling, D. Reidel Publishing Company, Dordrecht, Holland, 1-36, 1982.

Campbell, G.S. and B.D. Tanner, `A Krypton Hygrometer for Measurement of Atmospheric Water Vapor Concentration', Proceedings of the 1985 International Symposium on Moisture and Humidity, Washington, D.C., 609-614, 1985.

Chiba, O., Stability dependence of the vertical velocity skewness in the atmospheric surface layer, J. Met. Soc. Japan, 56, 140-142, 1978.

Denmead, O.T. and E.F. Bradley, `Flux-Gradient Relationships in a Forest Canopy', in B.H. Hutchinson and B.B. Hicks (eds.), The Forest - Atmospheric Interaction, D. Reidel Publishing Company, Dordrectt, Holland, 421-442.

Fisch, G., Armazenamento e Fluxos de Energia sobre Floresta da Amazonia Central, M.Sc. Thesis, University of Sao Paulo, Brazil, 1986.

Harriss, R.C., S.C. Wofsy, M. Garstang, L.C.B. Molion, R.J. McNeal, J.M. Hoell, R.J. Bendura, S.M. Beck, R.L. Navarro, J.T. Riley, R.L. Snell, `The Amazon Boundary Layer Experiment', submitted to J. Geophys. Res., 1987.

Huagen, D.A., J.C. Kaimal, and E.F. Bradley, `An Experimental Study of Reynolds Stress and Heat Flux in the Atmospheric SFC Layer', Quart. J.R. Met. Soc., 97, 168-180, 1971.

Hicks, B.B., `Propeller Anemometers as Sensors of Atmospheric Turbulence', Boundary-Layer Meteorol., 3, 214-228, 1972.

Jarvis, P.G., G.B. James and J.J. Landsberg, `Coniferous Forest', in Vegetation and the Atmosphere, Vol. II (J.L. Monteith, Ed.), Academic Press (London), 1976.

Kaimal, J.C. and J.E. Gaynor, `The Boulder Atmospheric Observatory', J. Appl. Met., 5, 863-880, 1983.

Lenschow, D.H. and L. Krisetnsen, `Uncorrelated Noise in Turbulence Measurements', J. Atmos. and Ocean. Tech., 2, 68-81, 1985.

Martin, C., D.R. Fitzjarrald, M. Garstang, and A.P. Oliveira, `Boundary-Layer Structure Observed Above the Tropical Forest', submitted to J. Geophys. Res., 1987.

McMillen, R.T., `A Basic Program for Eddy Correlation in Non-simple Terrain', NOAA Technical Memorandum ERL/ASL-147, 32 pp., 1986.

Moore, C.J., `Frequency Response for Eddy Correlation Systems', Boundary-Layer Meteorol., 37, 17-36, 1986.

Panofsky, H.A. and J.A. Dutton, Atmospheric Turbulence, John Wiley & Sons, Inc., Canada, 161 pp., 1984.

Raupach, M.R., `Anomalies in Flux-Gradient Relationships over Forest, Boundary-Layer Meteorol., 16, 467-486, 1979.

Raupach, M.R., A Lagrangian analysis of scalar transfer in vegetation canopies, Q. J. Roy. Met. Soc., 113, 107-120, 1987.

Raupach, M.R. and A.S. Thom, `Turbulence in and Above Plant Canopies', Annual Review of Fluid Mechanics, 13, 97-129, 1981.

Shuttleworth, W.J., J.H.C. Gash, C.R. Lloyd, C.J. Moore, J. Roberts, A.DeO.M. Filho, G. Fisch, V.DeP.S. Filho, M.DeN.G. Ribeiro, L.C.B. Molion, L.D.DeA. Sa, J.C.A. Nobre, O.M.R. Cabral, S.R. Patel, J.C. DeMoraes, `Eddy Correlation Measurements of Energy Partition for Amazonian Forest', Quart. J. Roy. Meteorol. Soc., 110, 1143-1162, 1984.

Shuttleworth, W.J., J.H.C. Gash, C.R. Lloyd, C.J. Moore, J. Roberts, A.DeO.M. Filho, G. Fisch, V.DeP.S. Filho, M.DeN.G. Ribeiro, L.C.B. Molion, L.D.DeA. Sa, J.C.A. Nobre, O.M.R. Cabral, S.R. Patel, J.C. DeMoraes, `Daily Variations of Temperature and Humidity Within and Above Amazonian Forest, Weather, 40(4), 102-108, 1985.

Shuttleworth, W.J. and Calder, Has the Priestley-Taylor Equation any Relevance to Forest Evaporation?, J. Appl. Met., 18, 639-646, 1979.

Silva Dias, P.L., W.H. Schubert, and M. DeMaria, `Large-Scale Response of the Tropical Atmosphere to Transient Convection', J. Atm. Sci., 40, 2689-2707, 1983.

Tanner, B.D., M.S. Tanner, W.H. Dugas, E.C. Campbell, and B.L. Bland, `Evaluation of an Operational Eddy Correlation System for Evapotranspiration Measurements', National Conference on advances in Evapotranspiration for the American Society of Agricultural Engineers, Chicago, IL, 1985.

Tillman, J.E., `The Indirect Determination of Stability, Heat and Momentum Fluxes in the Atmospheric Boundary Layer from Simple Scalar Variables During Dry Unstable Conditions', J. Appl. Meteorol., 11, 783-792, 1972.

Verma, S.B., D.D. Baldocchi, D.E. Anderson, D.R. Matt, and R.J. Clement, `Eddy Fluxes of CO_2, Water Vapor, and Sensible Heat over a Deciduous Forest', Boundary-Layer Meteorol., 36, 71-91, 1986.

Wesely, M.L., Eddy Correlation Measurements in the Atmospheric Surface Layer over Agricultural Crops, Ph.D. Thesis, Univ. of Wisconsin, 1970.

Wieringa, J., A Reevaluation of the Kansas Mast Influence on Measurements of Stress and Cup Anemometer Overspeeding, Boundary-Layer Meteorol., 18, 411-430, 1980.

Wyngaard, J.L., `On Surface-Layer Turbulence', in D.A. Haugen (ed.), Workshop on Micrometeorology, Amer. Met. Soc., 101-149, 1973.

Wyngaard, J.C., `Cup, Propeller, Vane, and Sonic Anemometers in Turbulence Research', Annual Review of Fluid Mechanics, 13, 399-423, 1981.

Wyngaard, J.C., Boundary-Layer Modelling, in Nieuwstadt, F.T.M., VanDop, H., Atmospheric Turbulence and Air Pollution Modelling, 69-106, D. Reidel Publishing Co., Dordrecht, Holland, 1982.

TABLE 1.

Variables archived by the data acquisition systems

<u>PDP 11/73 system:</u>

Archived at the both top (45 m) and bottom (39 m) levels

σ_w σ_T σ_q $\overline{wT}$ $\overline{wq}$ $\overline{w^2T}$ $\overline{w^2q}$ $\overline{wT^2}$ $\overline{wq^2}$ $\overline{w^3}$ $\overline{Tq}$

Archived at top (=1) and bottom (=2)

$\overline{w_1 u_{Gill}}$ $\overline{w_1 w_2}$ $\overline{T_1 T_2}$ $\overline{q_1 q_2}$ u_{Gill} Φ_{Gill}

Note: Power spectra were archived
for w, T, and q at each level. Cospectra and quadrature spectra were
archived for all second moment quantities.

<u>Campbell Datalogger System</u>

σ_w σ_T σ_q $\overline{wT}$ $\overline{wq}$ $\overline{Tq}$ at each level.

FIGURE CAPTIONS

Figure 1. a) Typical examples of power spectra calculated and archived each twenty minutes for instruments at the 45 m level: vertical velocity (w), temperature (T), humidity (q), and horizontal wind speed as measured by the Gill anemometer (Gill). The dashed line represents a least-squares fit to the higher frequency data with the slope predicted for an inertial subrange.

b) Typical examples of hourly-averaged cospectra. The linear abscissa is arbitrary; horizontal line marks zero.

Figure 2. Comparison of the measured sensible heat fluxes at 39 m and at 45 m over twenty-minute periods. The plotted number represents the quadrant from which the wind came during each period (meteorological coordinates): [0°-90°] = 1; [91°-180°] = 2; [181°-270°] = 3; [271°-359°] = 4. Note that the instrument at 45 m faces toward the east; the one at 39 m faces toward the south.

Figure 3. Values of sensible heat flux calculated using the PDP data acquisition system (O) and with the Datalogger system (X). Values from the Hydra are marked with 'H': a) July 26; b) July 25.

Figure 4. Hourly averages of the momentum flux obtained with the top sonic anemometer and the Gill propeller vane ($\sqrt{-uw}$, m/s) compared with the scaled standard deviation of w at that level ($\sigma_w/1.25$). The number

plotted indicates the date when the hourly average was obtained (5 = 7/25, etc.). Data from the Hydra are marked with 'H'.

Figure 5. Estimates of the characteristic length scale calculated using the relation $\ell = u_*^3/\kappa\epsilon$ as a function of the buoyant production rate at the 45 m level, (g/θ_0) wT, for

a) u_* estimated using the sonic anemometer w and Gill anemometer u covariance and b) $u_* = \sigma_w/1.25$.

The number plotted indicates the date when the hourly average was obtained (5 = 7/25, etc.).

Figure 6. Hourly values of a) temperature and b) specific humidity (solid) with saturation specific humidity (+) averaged over the period 30 July through 5 August 1985 at the 45 m level of the tower.

Figure 7. a) Hourly averages of σ_q, σ_T, and σ_w at the 45 m level (solid) and the 39 m level (dashed) for the period 30 July through 5 August 1985.

b) Hourly averages of the correlation coefficients between T and q (R_{Tq}), between w and q (R_{wq}), and between w and T (R_{wT}) at the 45 m level (solid) and the 39 m level (dashed) for the period 30 July through 5 August 1985.

c) Hourly averaged heat budget for the period 30 July through 5 August 1985: Incoming solar radiation, S, (dotted), net radiation, R_n, (dash-dot with +), latent, LE, and sensible heat fluxes, H, at the 45 m level (solid), latent heat flux at the 39 m level (solid with +), with the residual $(H + LE - R_n)$ shown dashed for the 45 m level, dashed with + for the 39 m level.

Figure 8. Heat budgets for a) 7/25, b) 7/26, c) 7/30, d) 7/31, e) 8/1, f) 8/2, g) 8/3, h) 8/4, and i) 8/5. Legend is the same as for Figure 7c.

Figure 9. a) Heat budget for 7/24. Legend is the same as for Figure 7c.

b) Time series of the drag coefficient ($Cd \equiv u_*^2 / U^2$) for July 26 (symbol 6) and for July 24 (symbol 4).

c) Time series of detrended deviation ten-second average data for temperature (T'), humidity (q'), and vertical velocity (w') for the twenty minute period beginning at 1221.

d) Time series of detrended deviation ten-second average data for temperature (T'), humidity (q'), and vertical velocity (w') for the twenty minute period beginning at 1241.

e) Time series of deviation ten-second average data from the twenty-minute linear trend for temperature (T'), humidity (q'), and vertical velocity (w') for the twenty minute period beginning at 1301.

Figure 10. Time series of the vertical velocity skewness on a) July 24, b) July 25, and c) July 26 at the 45 m level (symbol 1) and the 39 m level

(symbol 2).

Figure 11. Budget of $\partial\sigma_w{}^2/\partial t$ shown for a) 24 July, b) 25 July and c) 26 July. Terms (as defined in the text) are: buoyant production (b); transport (t); dissipation (d); and the residual ($r \equiv b + t + d$).

Figure 12. Budget of $\partial\overline{w\theta}/\partial t$ for a) 25 July and b) 26 July. Terms are: buoyant production (b) and transport (t). Estimated value of the gradient production term for typical convective conditions is marked G. The estimated value of this term during a trasnient stable period on 26 July is marked with G', as discussed in the text.

A

7/25 1341

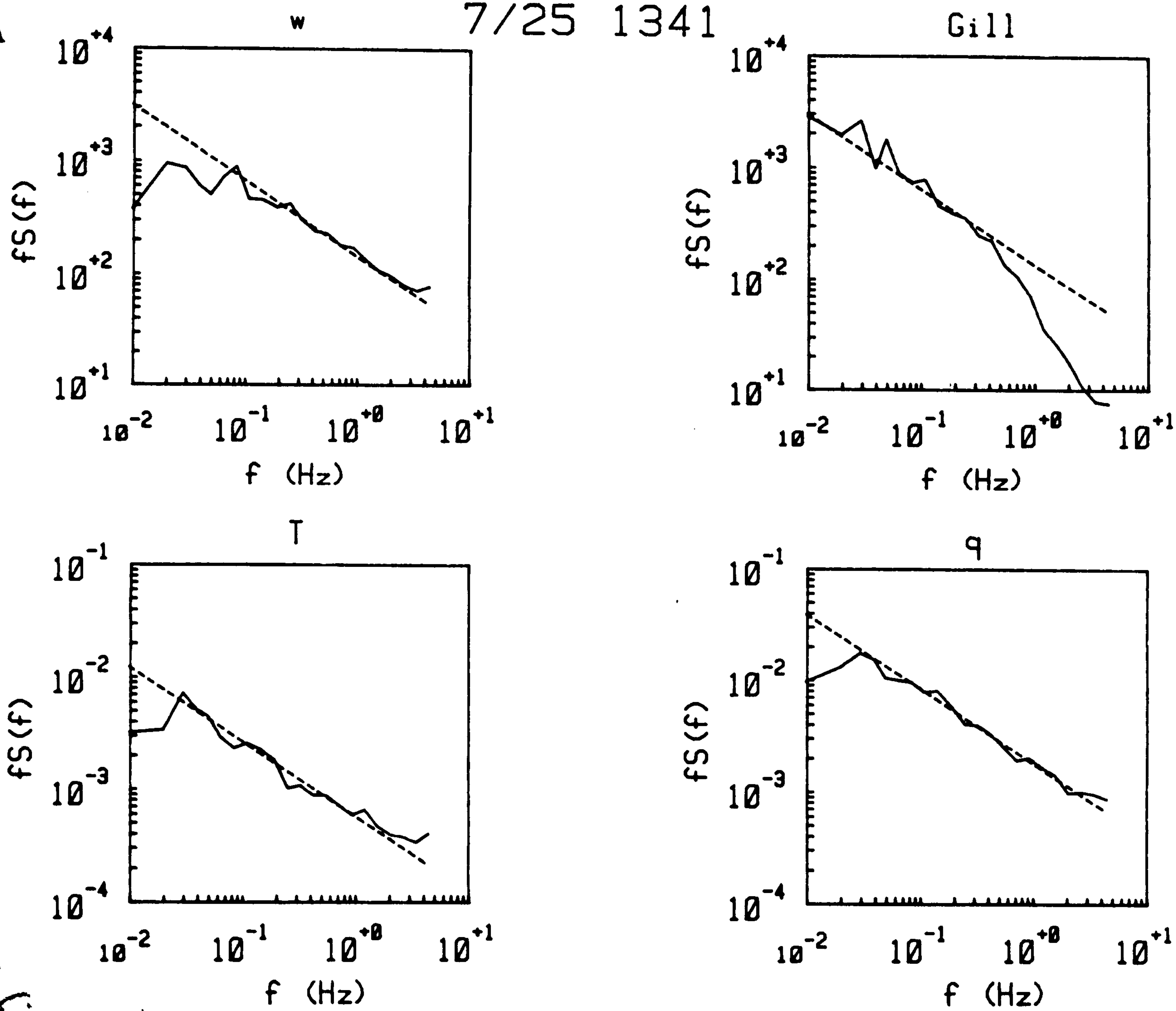

Fig 1A

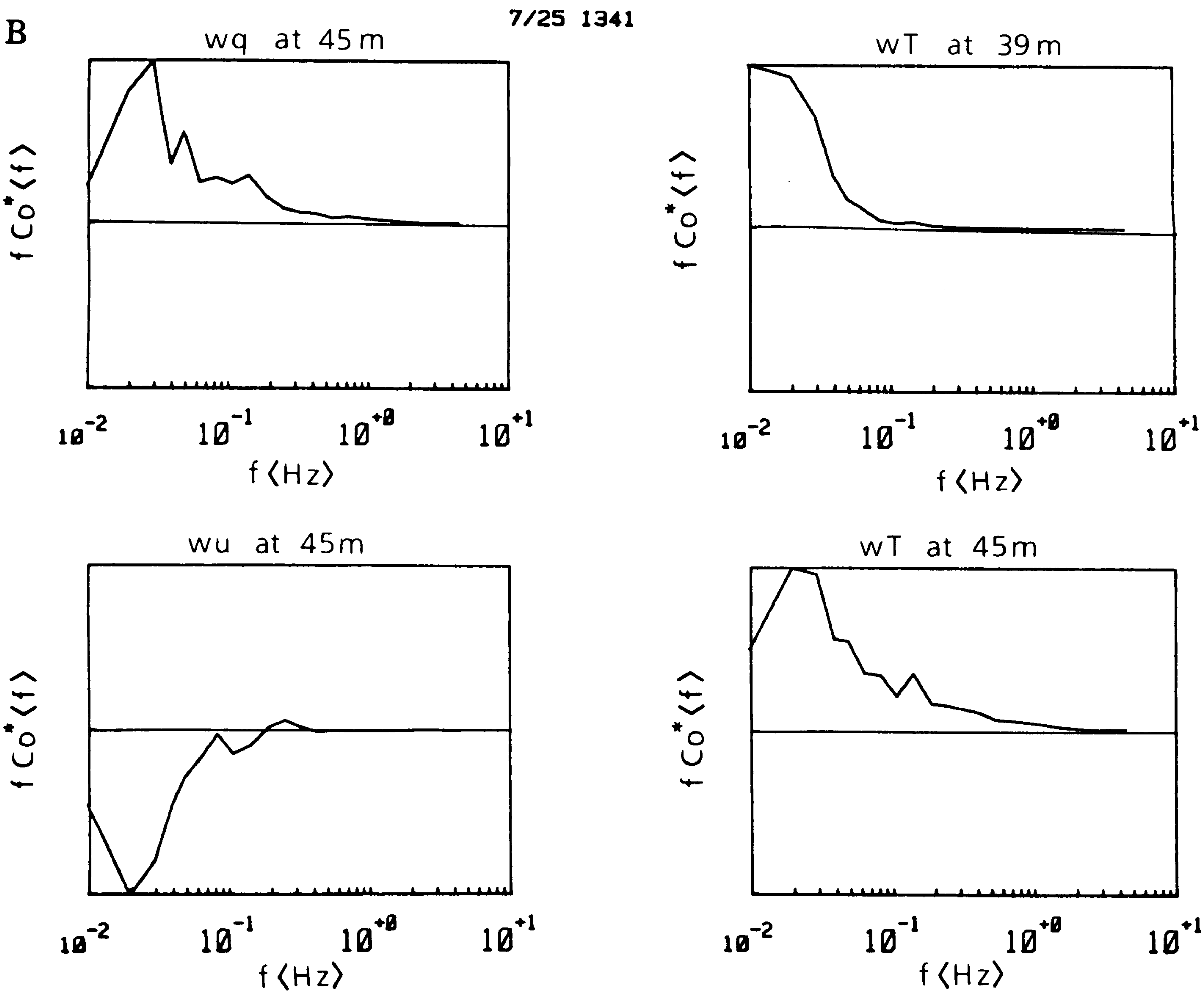
B
7/25 1341
wq at 45m
wT at 39m
wu at 45m
wT at 45m
f Co*(f)
f (Hz)
10^-2
10^-1
10^+0
10^+1

Fig. 1B

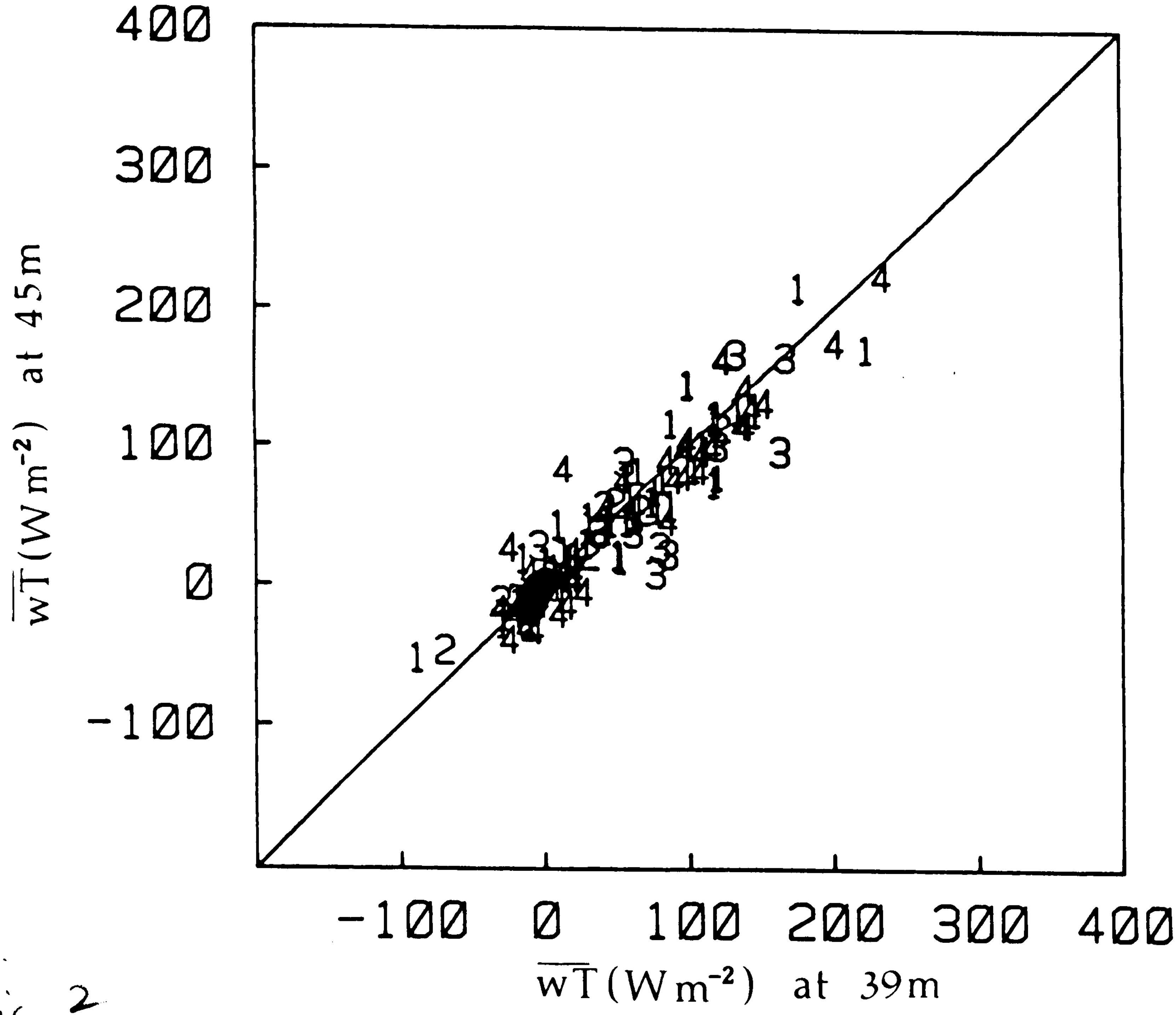
400
300
200
100
0
-100
$\overline{wT}$ ($W m^{-2}$) at 45m
-100
0
100
200
300
400
$\overline{wT}$ ($W m^{-2}$) at 39m

Fig 2

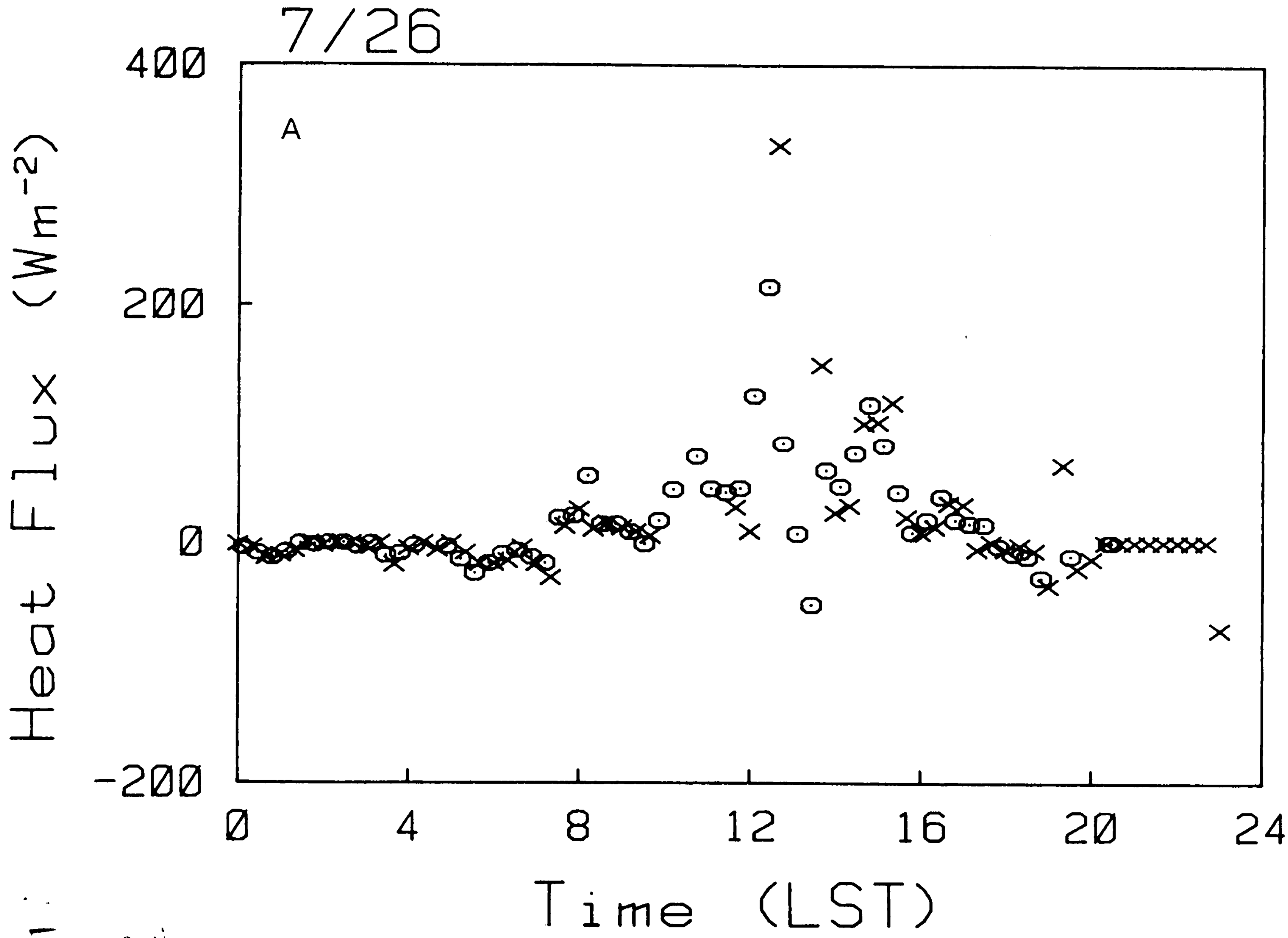

Fig. 3A

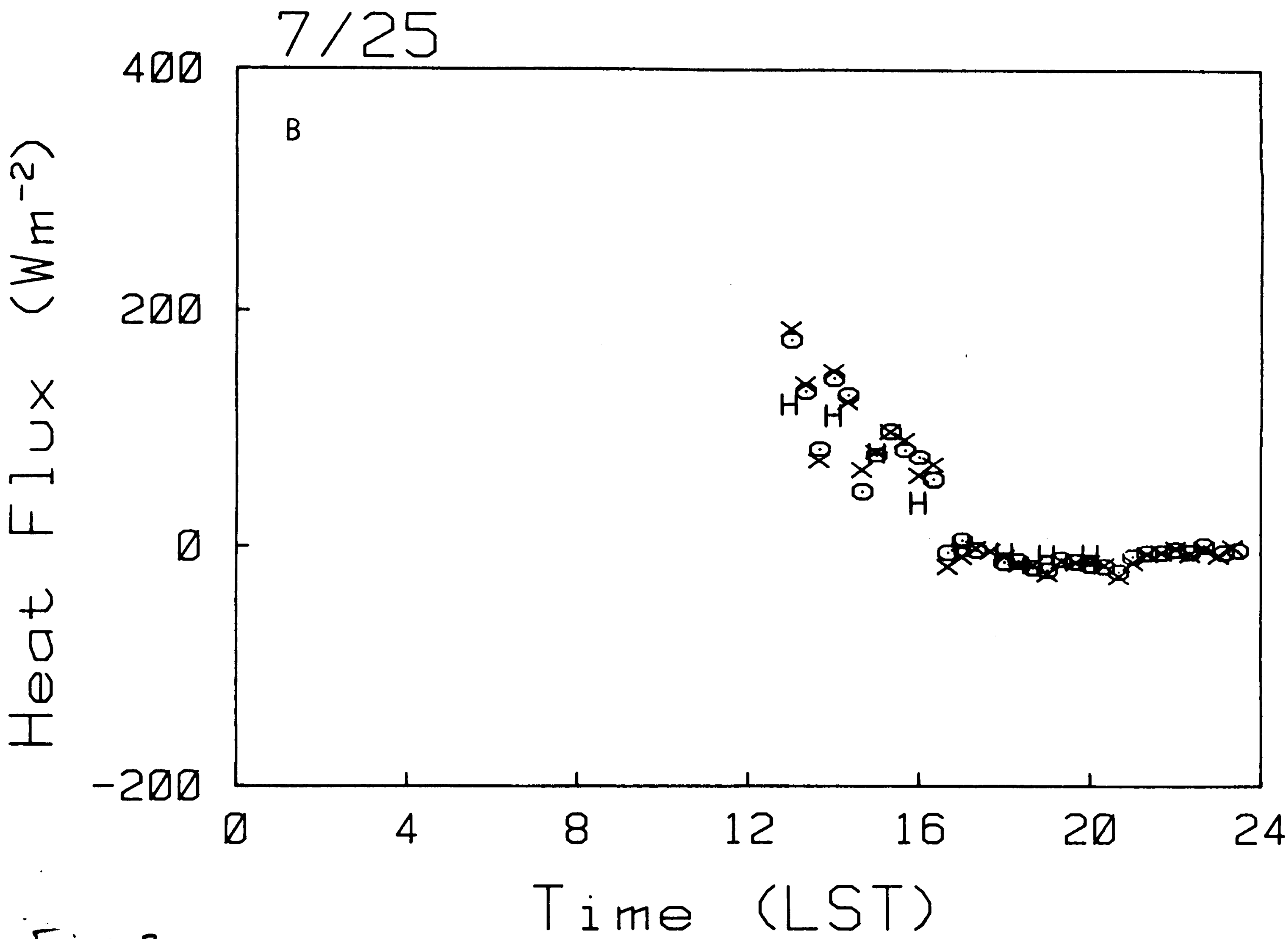

Fig 2 B

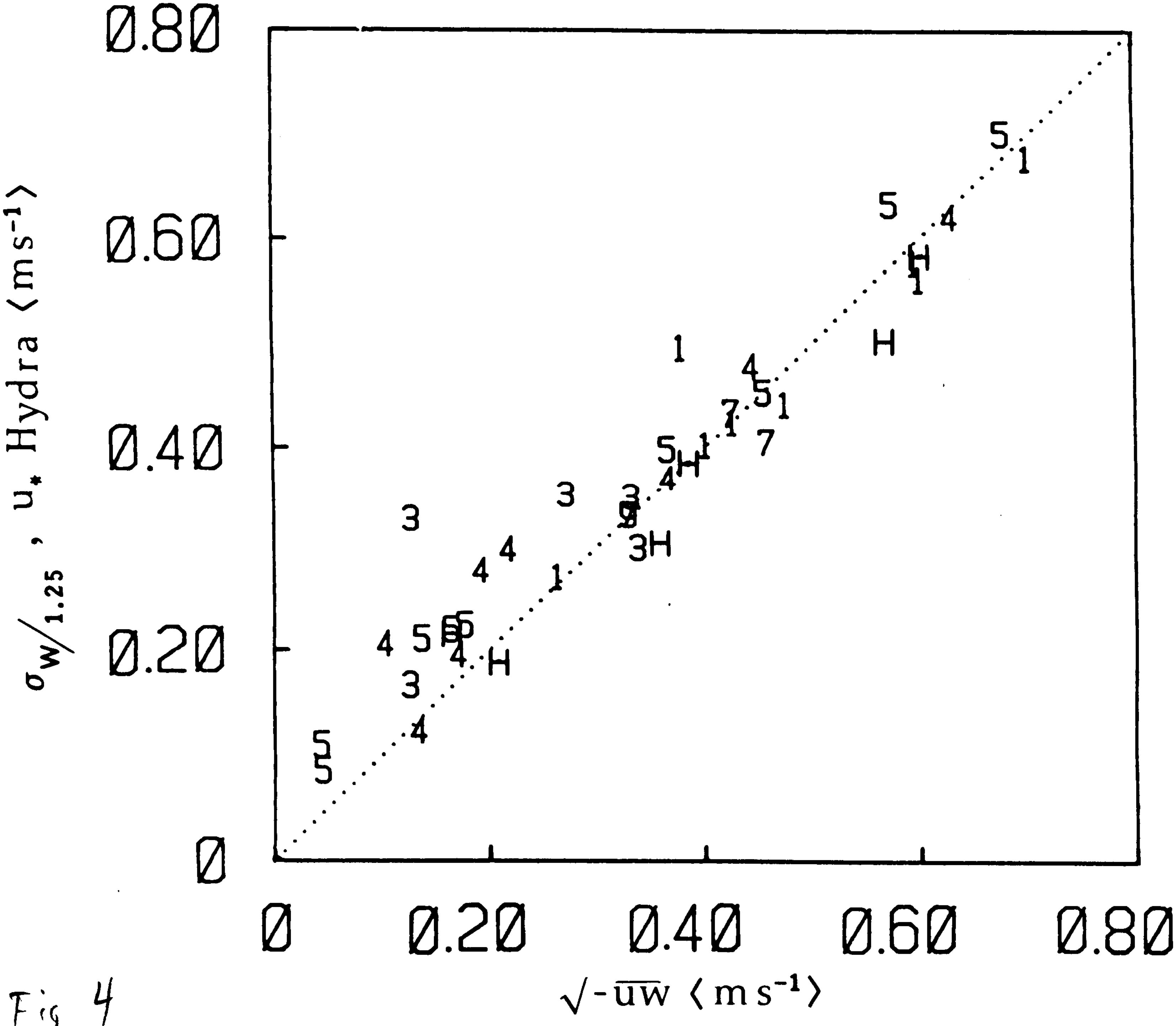

Fig 4

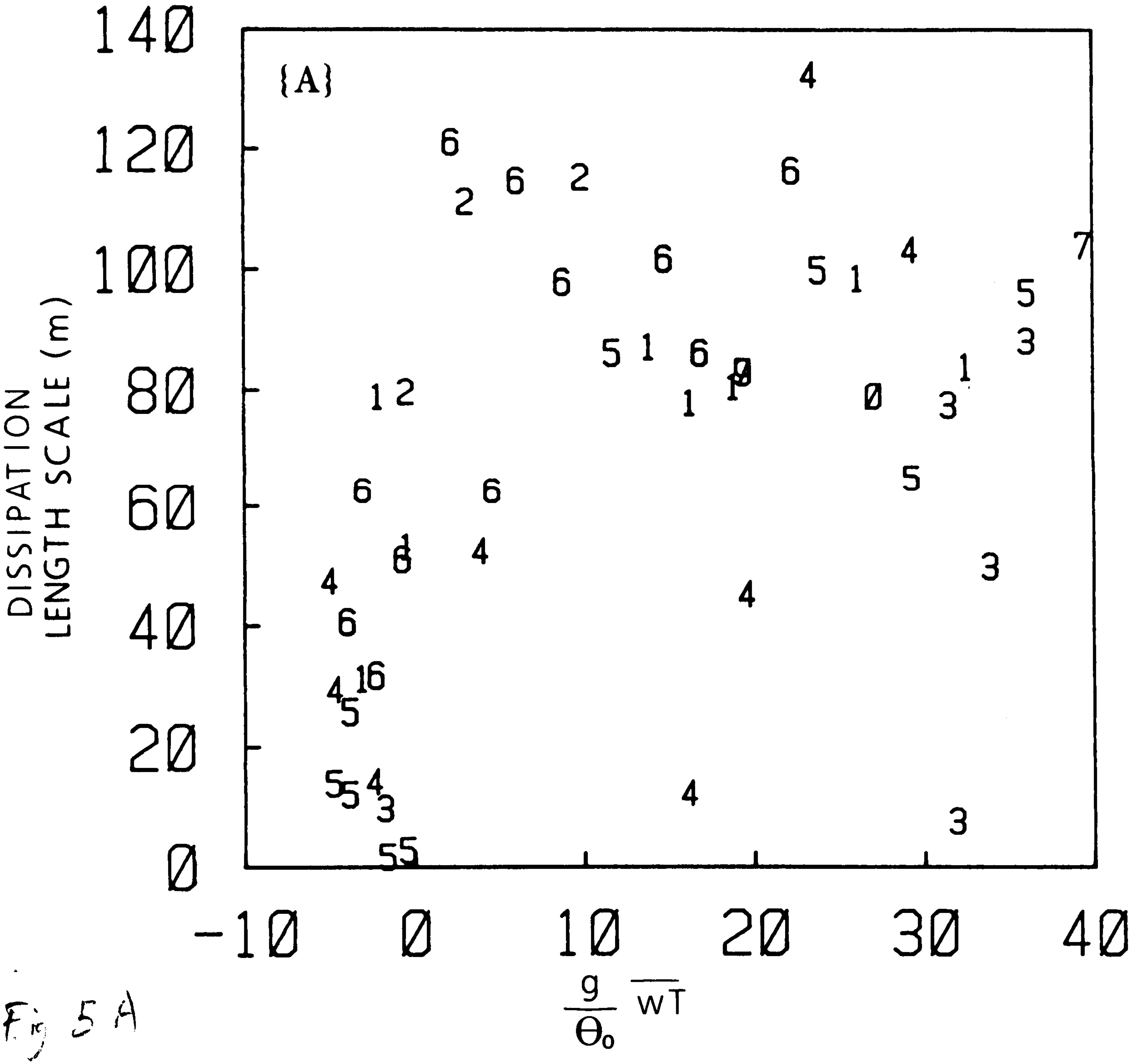

Fig 5A

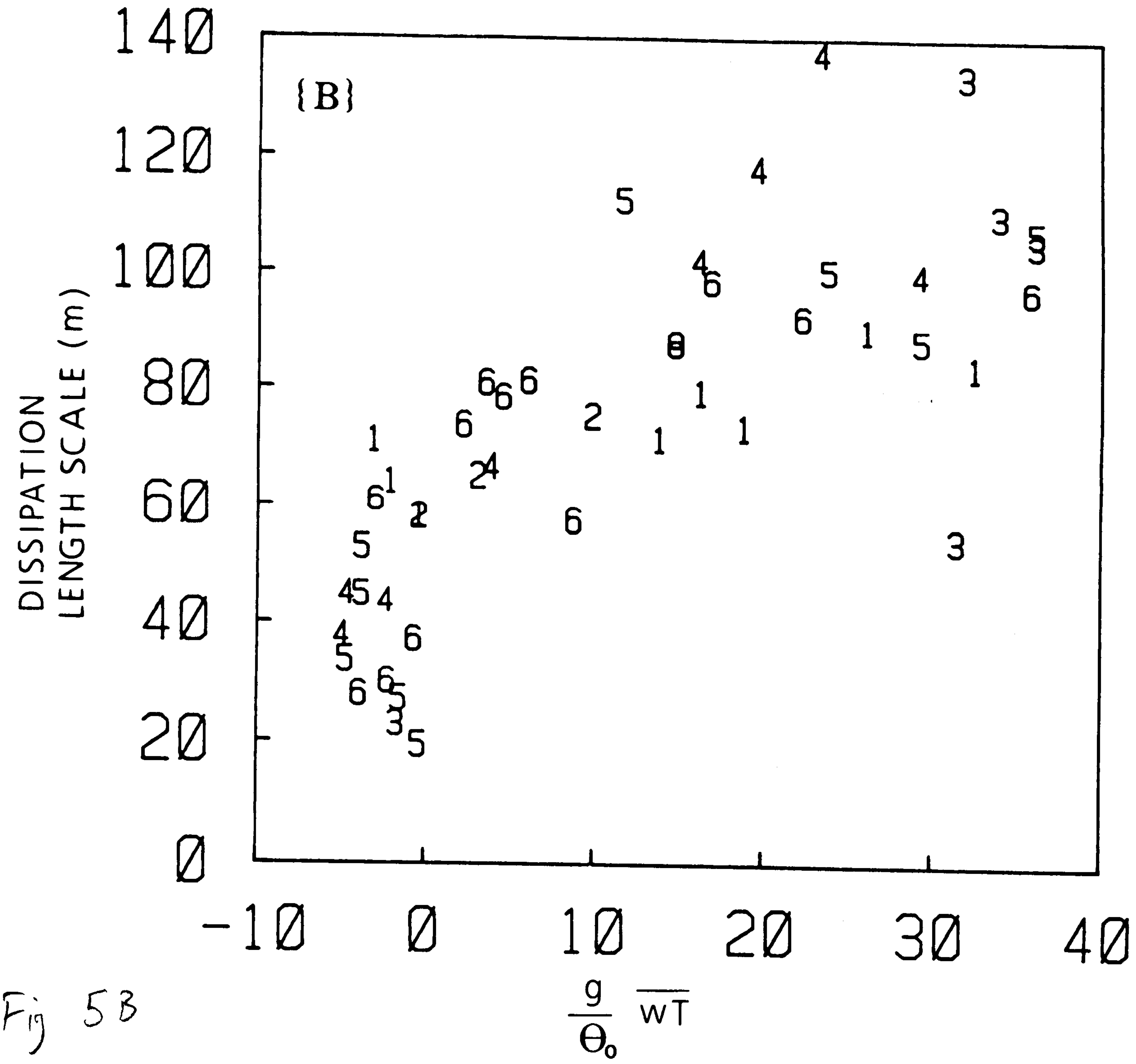
{B}
DISSIPATION
LENGTH SCALE (m)
140
120
100
80
60
40
20
0
-10
0
10
20
30
40
$\frac{g}{\Theta_o} \overline{wT}$

Fig 5B

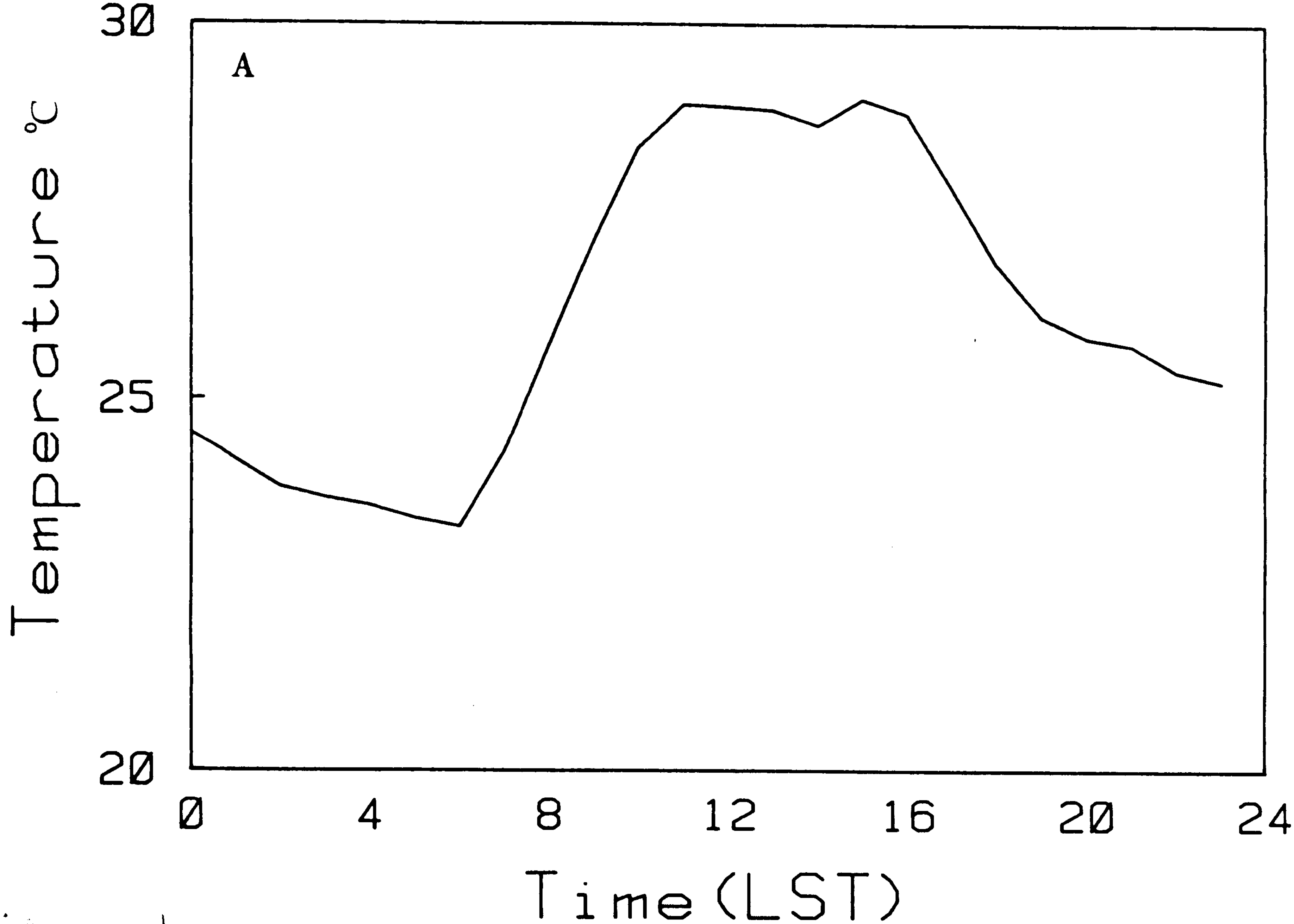

Fig 6A

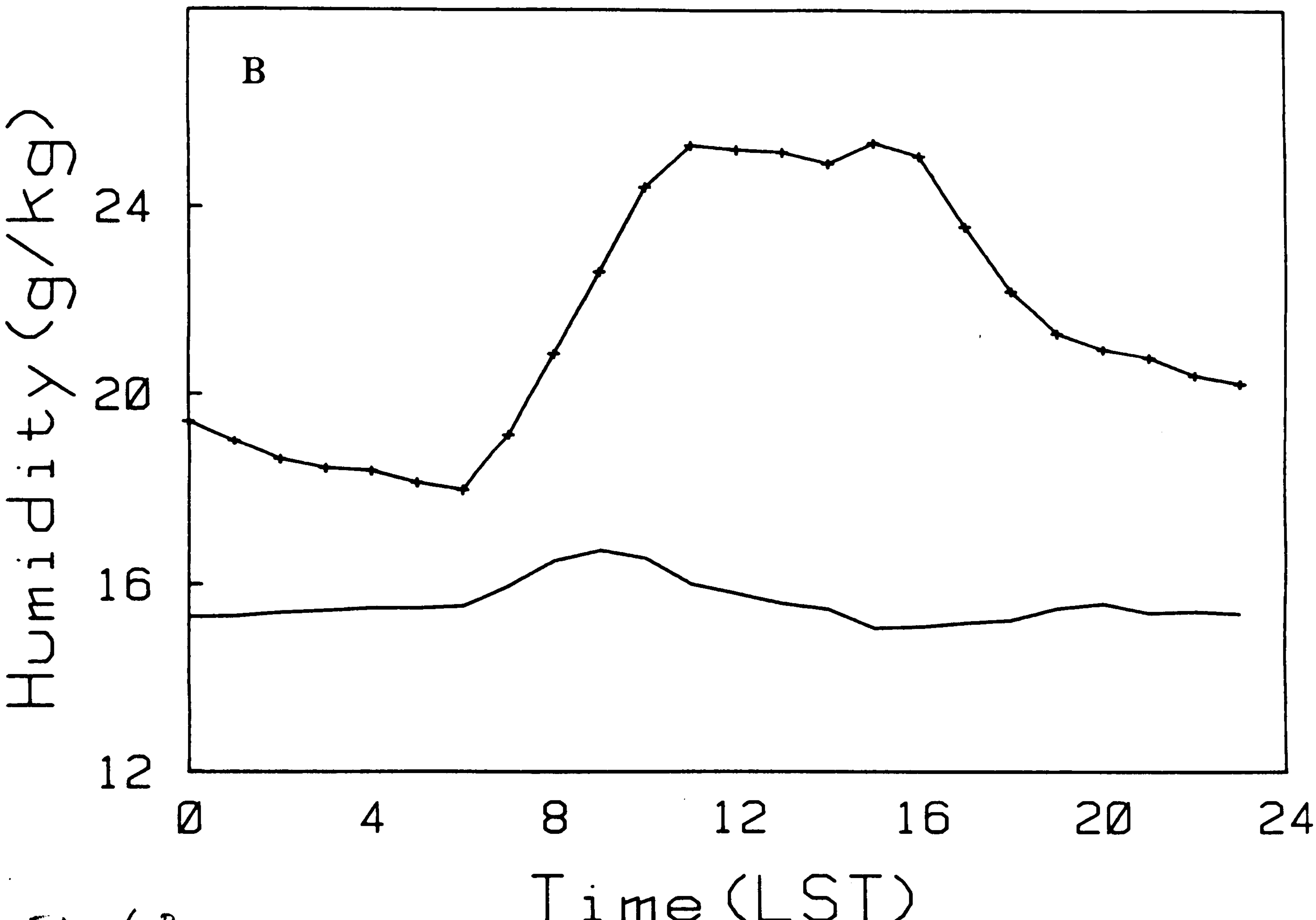

Fig 6B

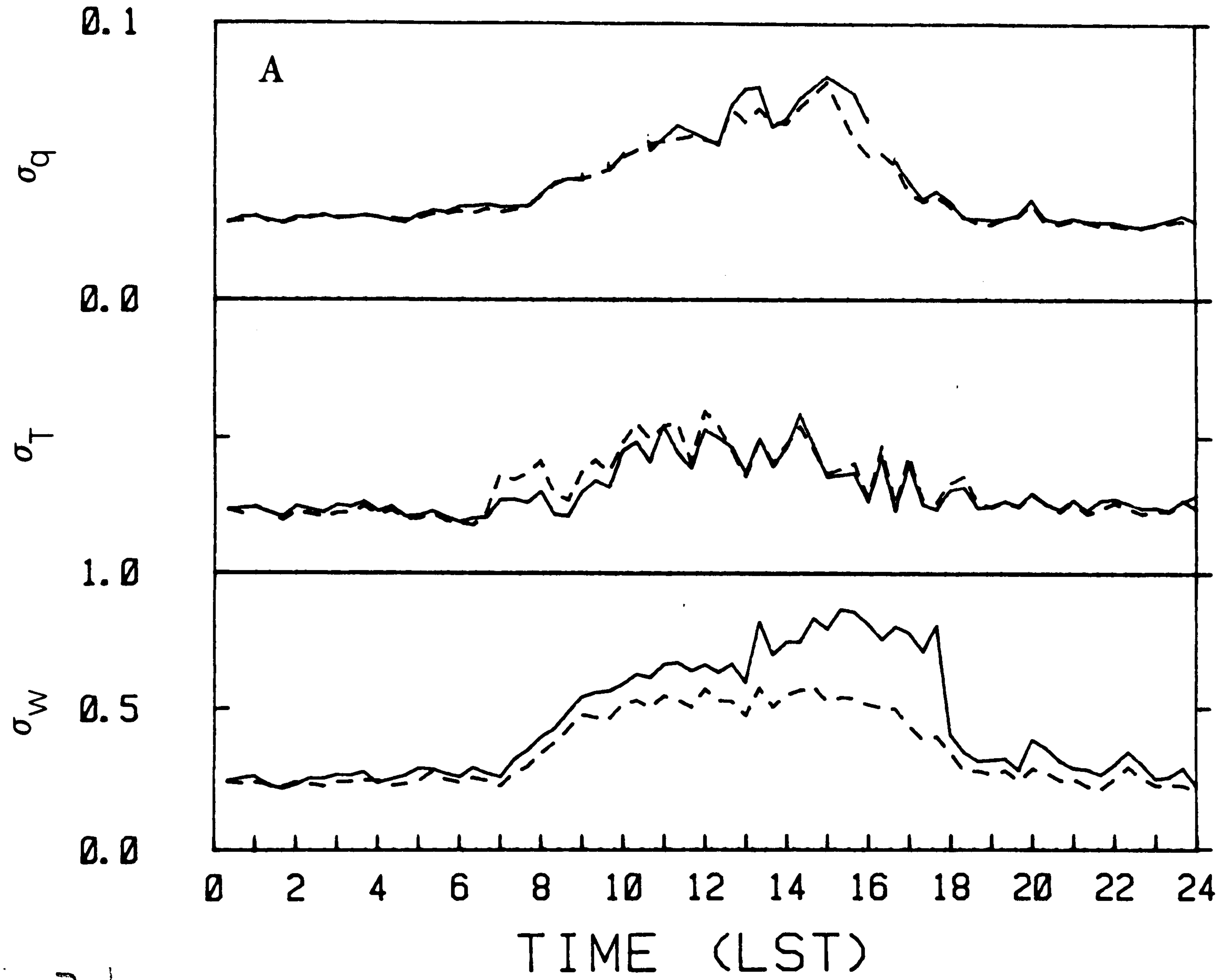

Fig 7A

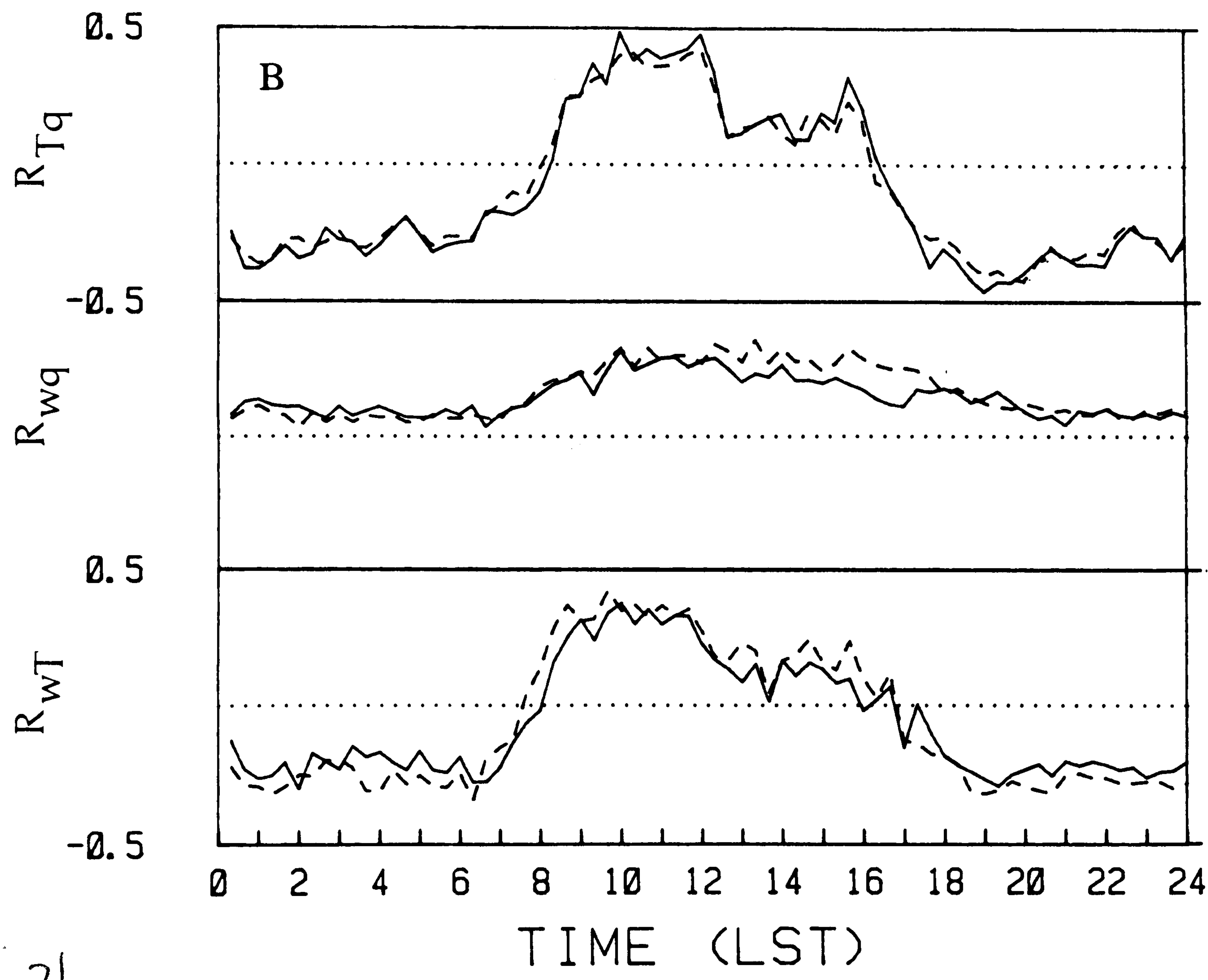

Fig. 7b

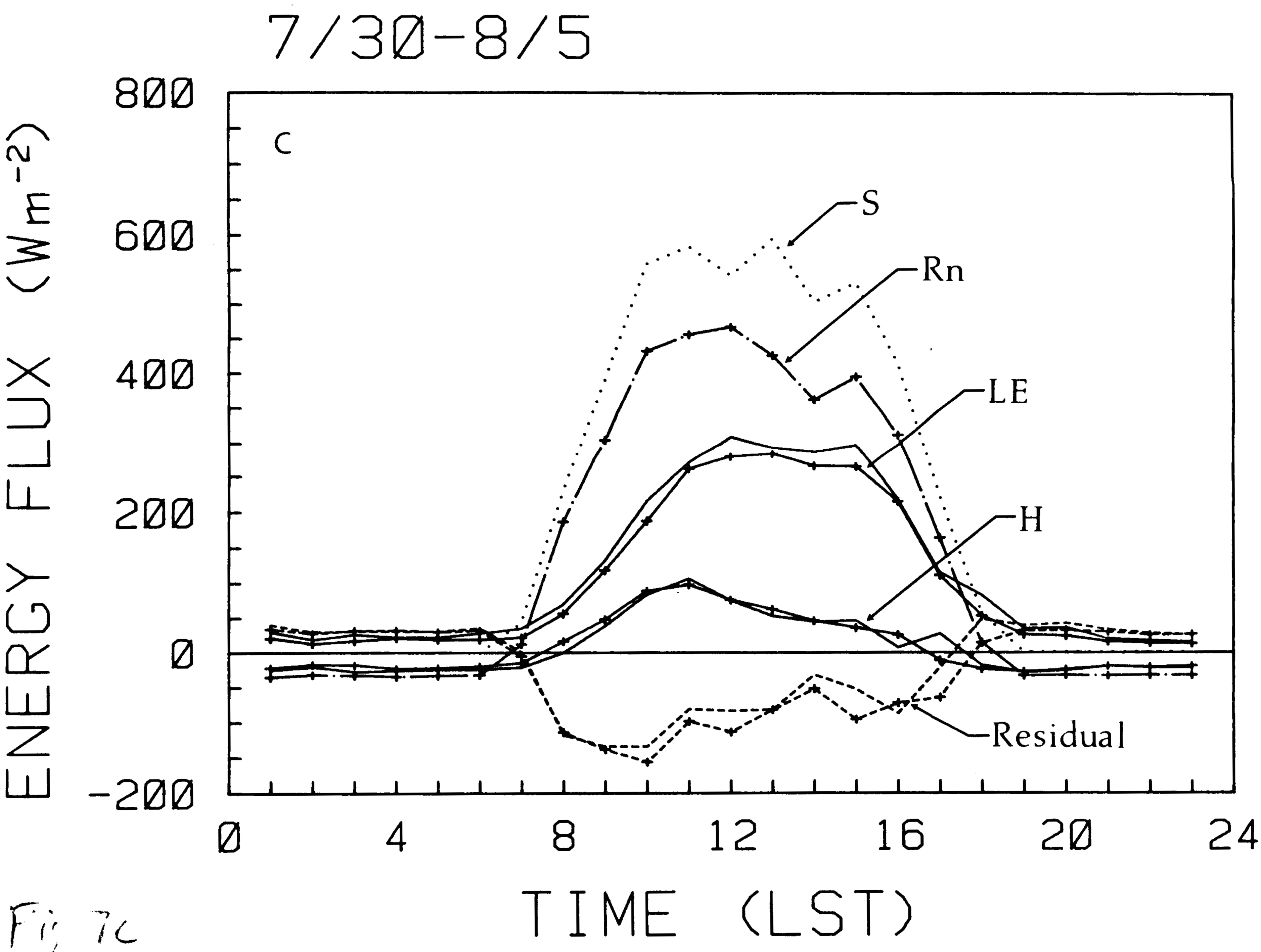

7/30-8/5
c
800
600
400
200
0
-200
ENERGY FLUX (Wm^-2)
0
4
8
12
16
20
24
TIME (LST)
S
Rn
LE
H
Residual

Fig 7c

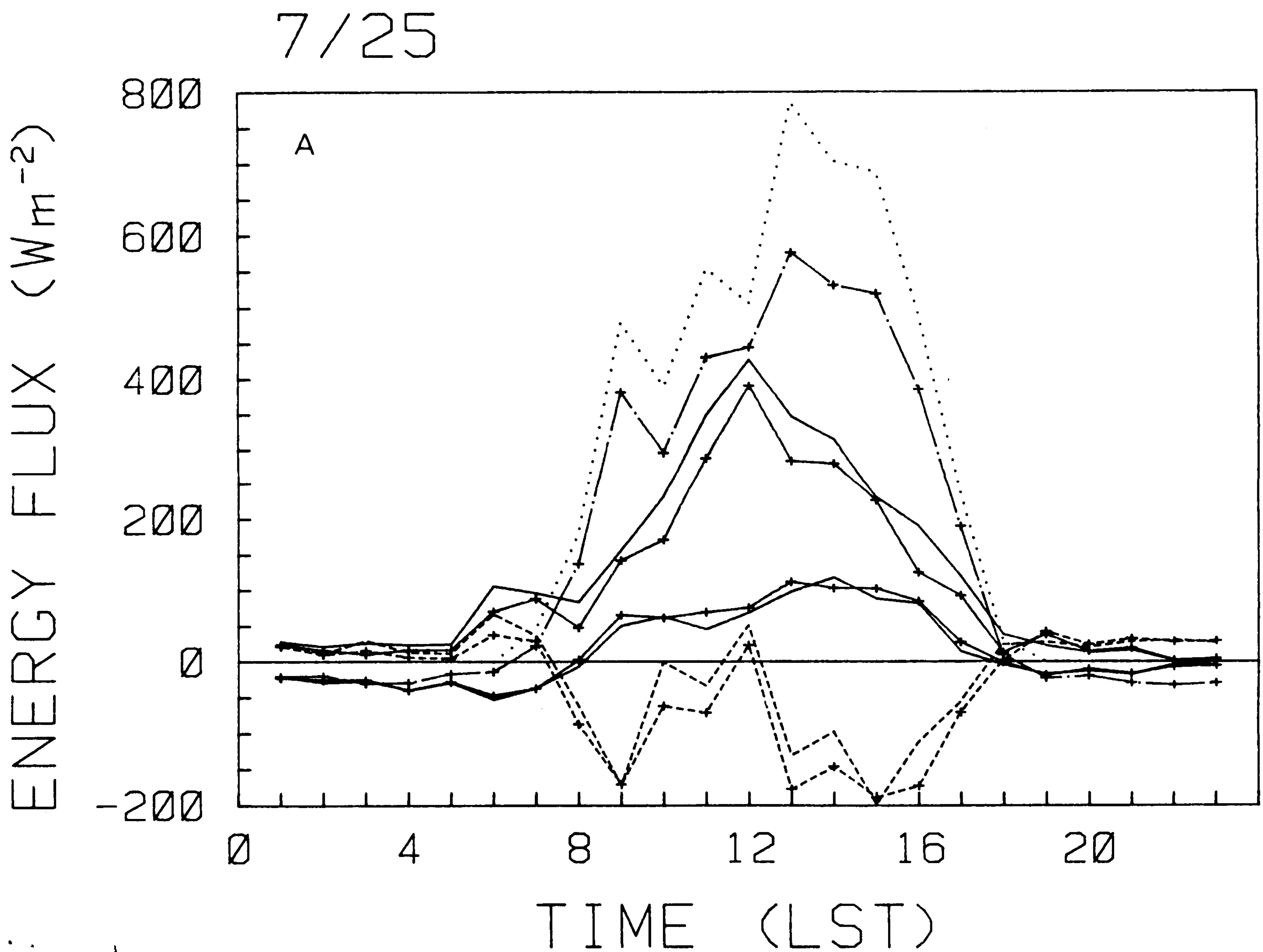

Fig 8A

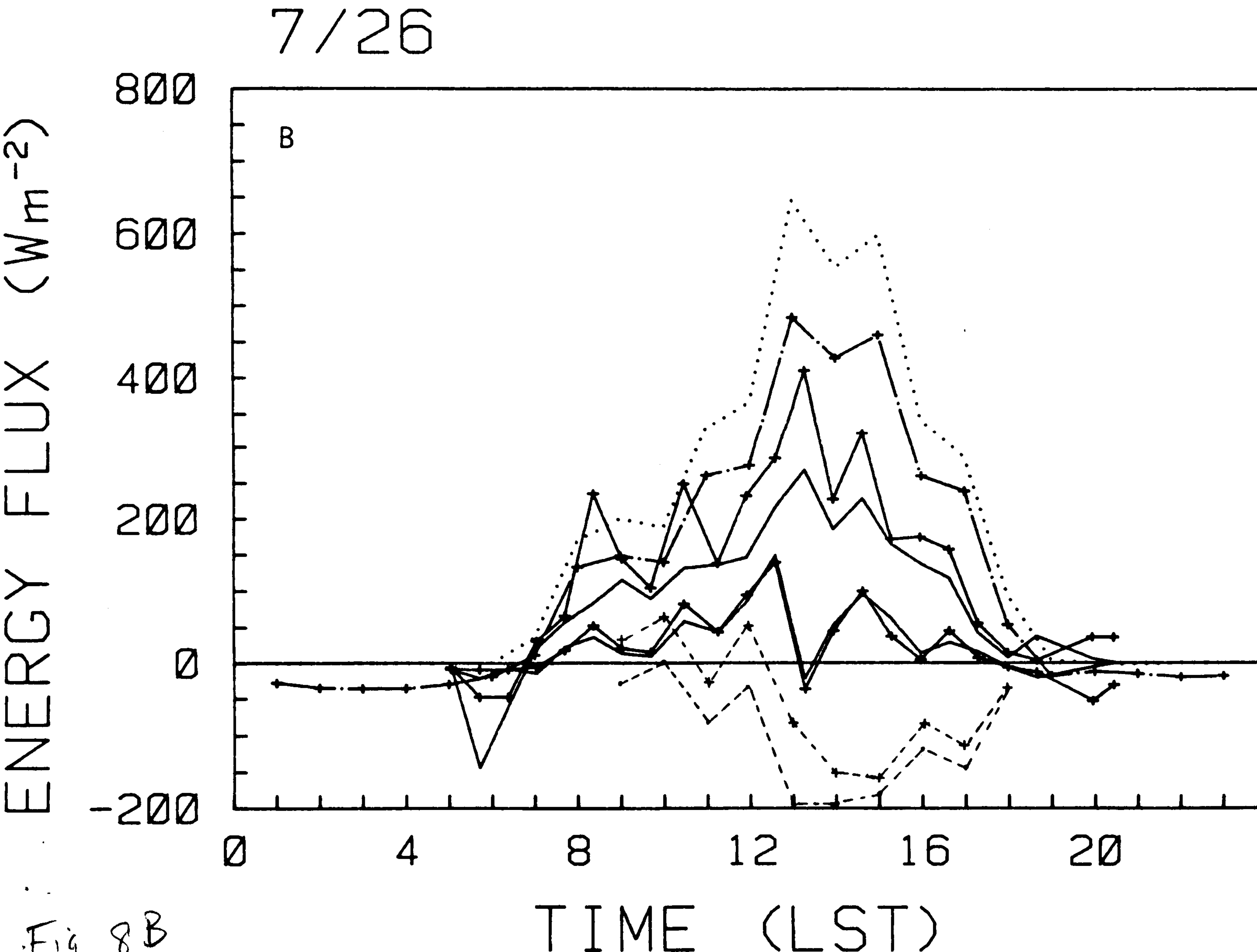

Fig 8B

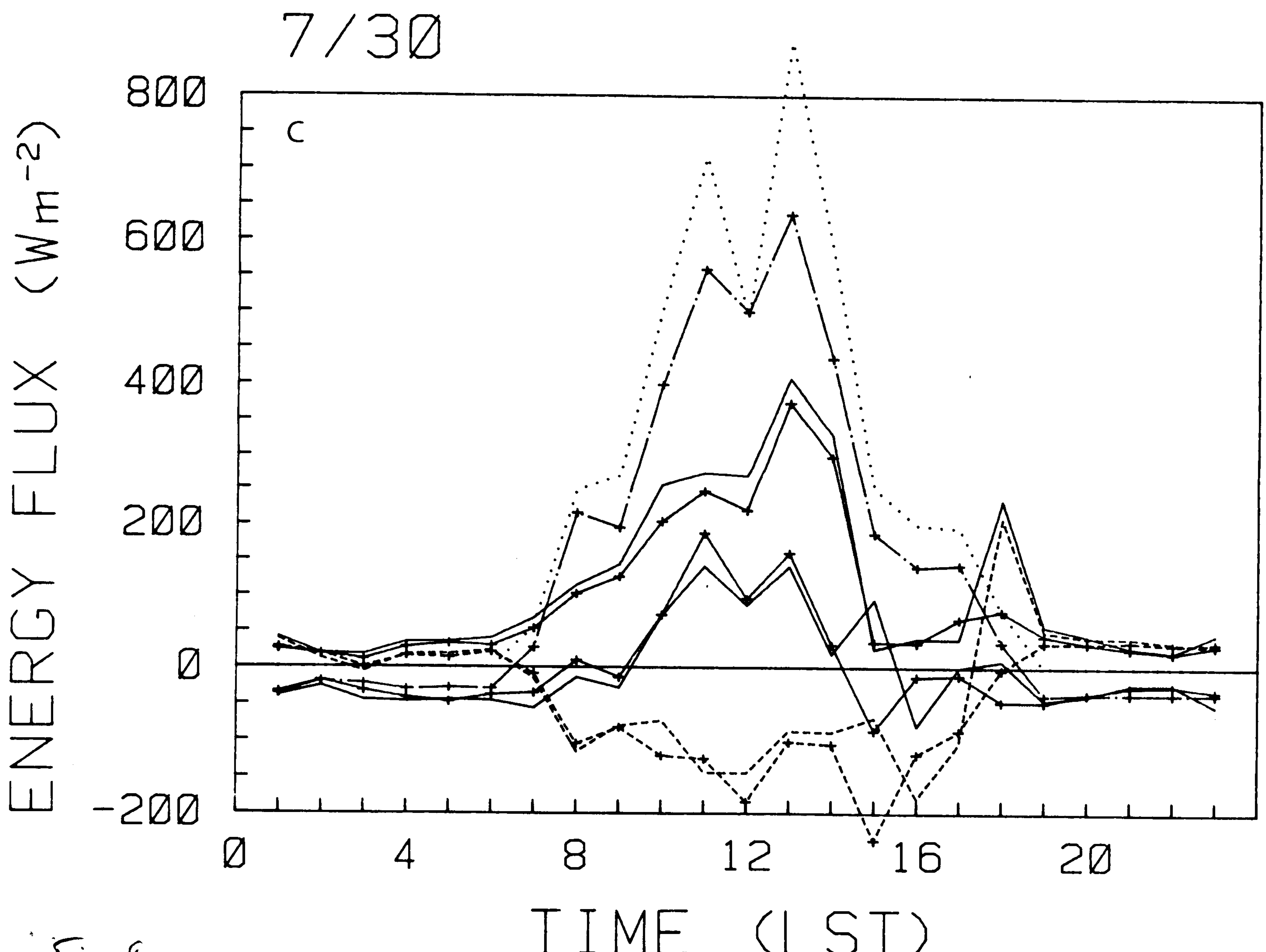

Fig 8c

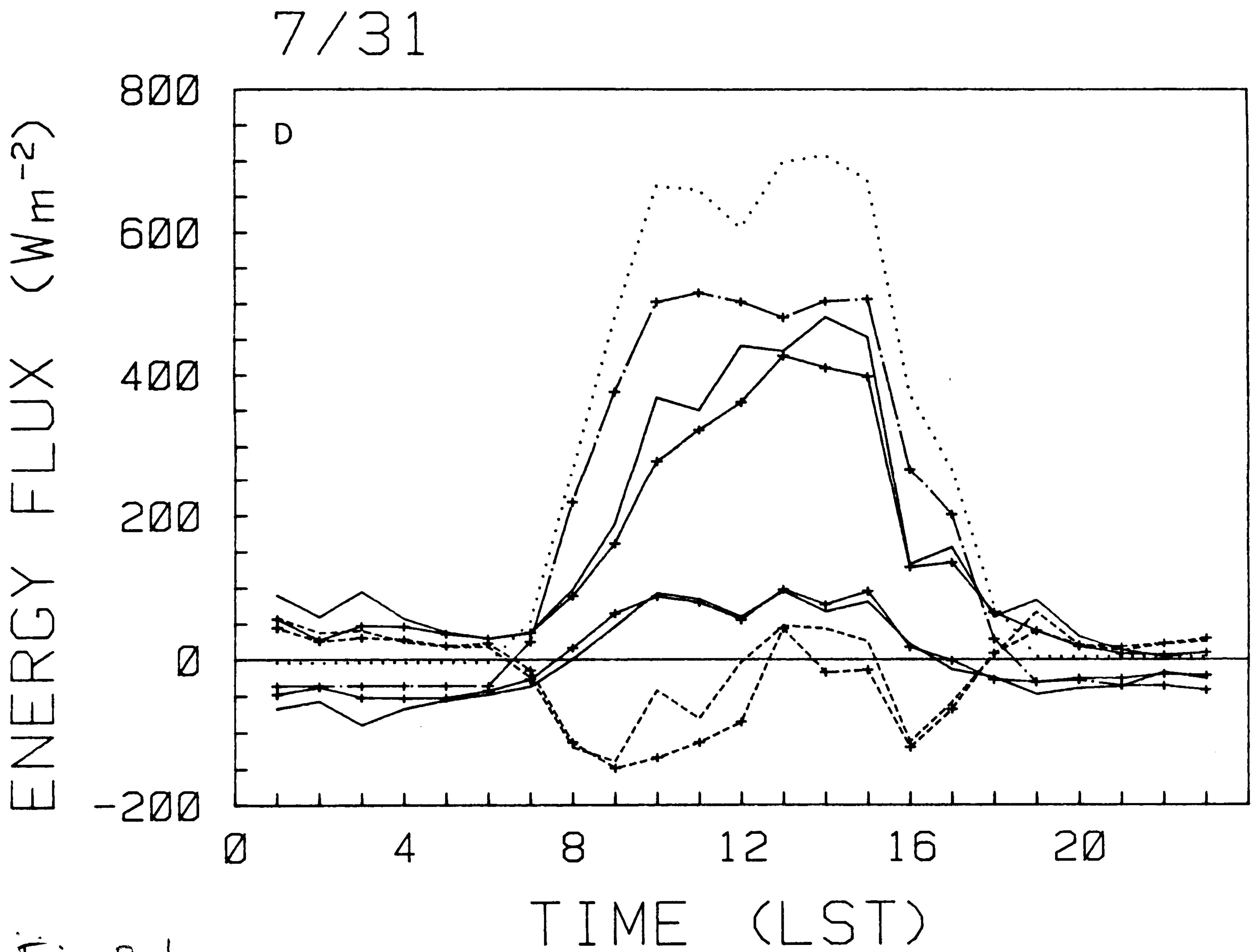

Fig 8d

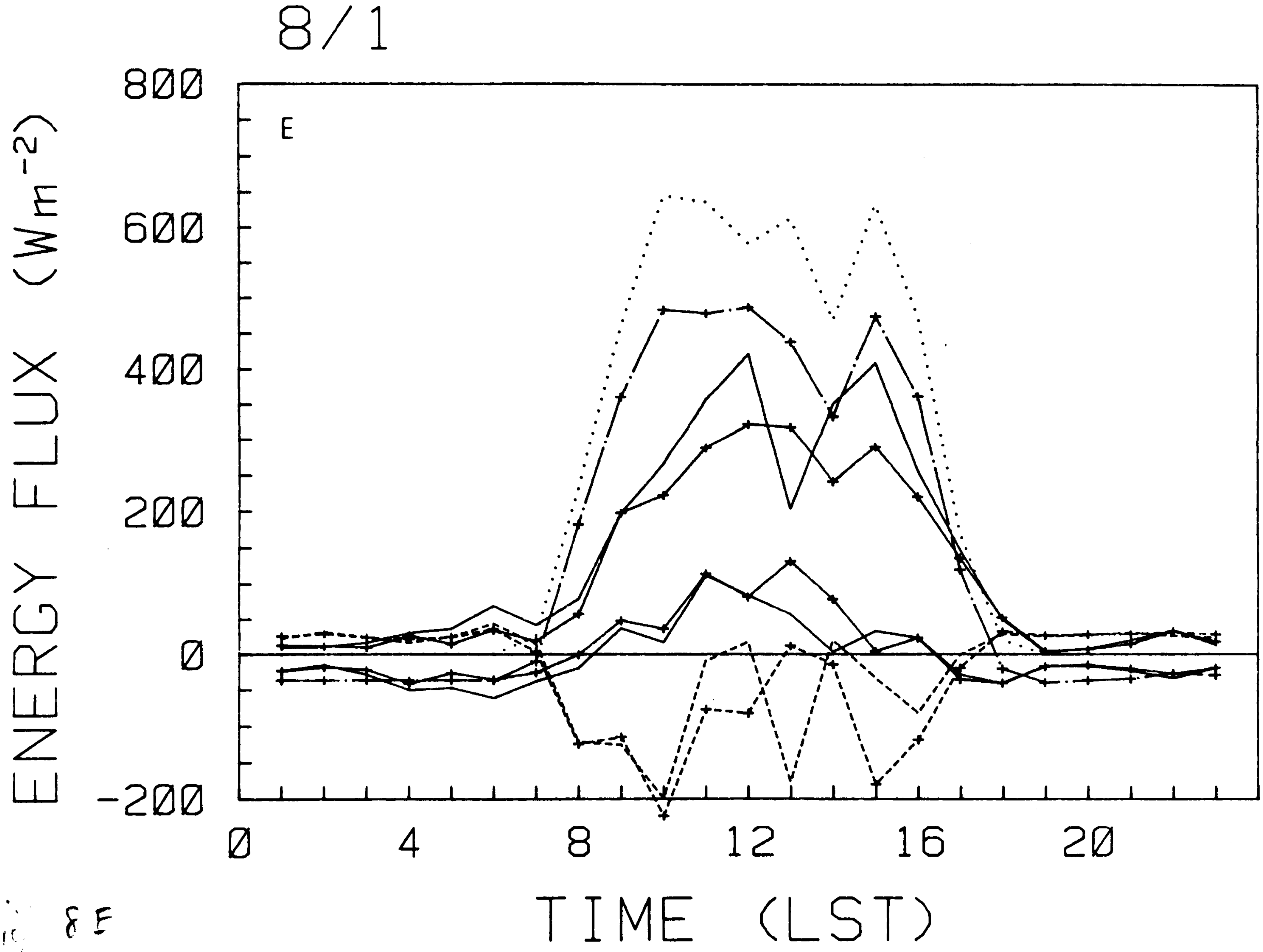

Fig. 8E

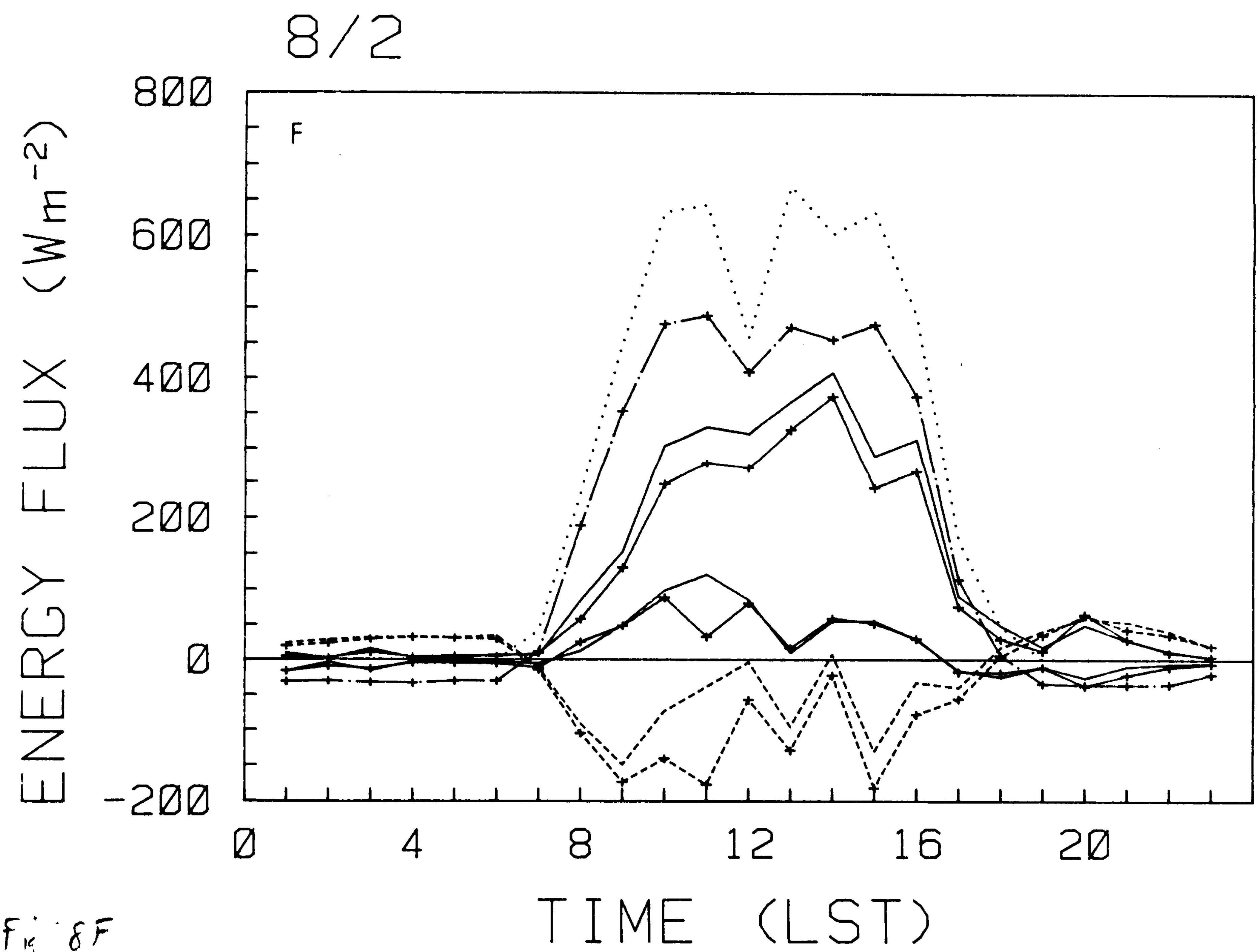

Fig 8F

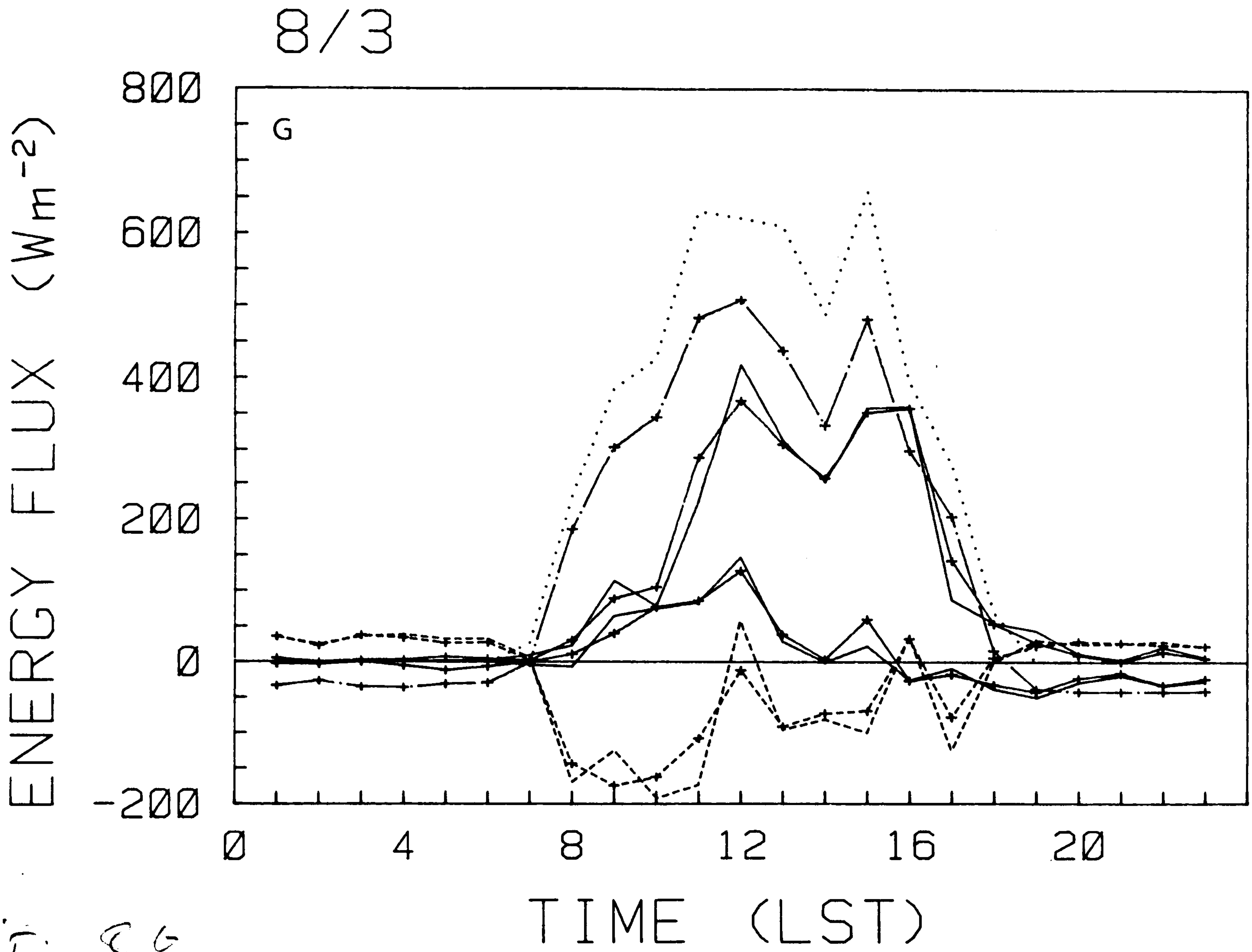

Fig 8 G

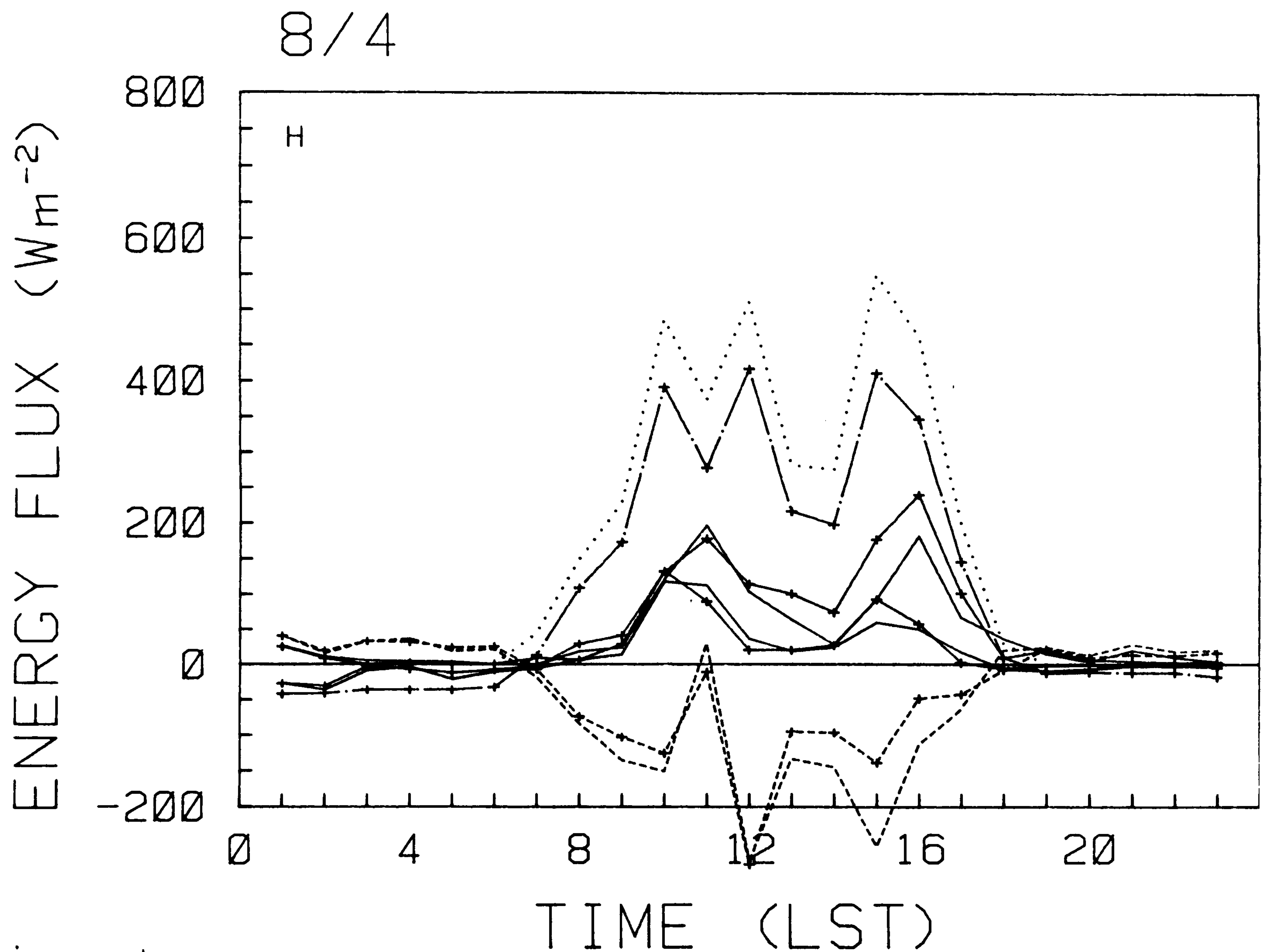

Fig 8 H

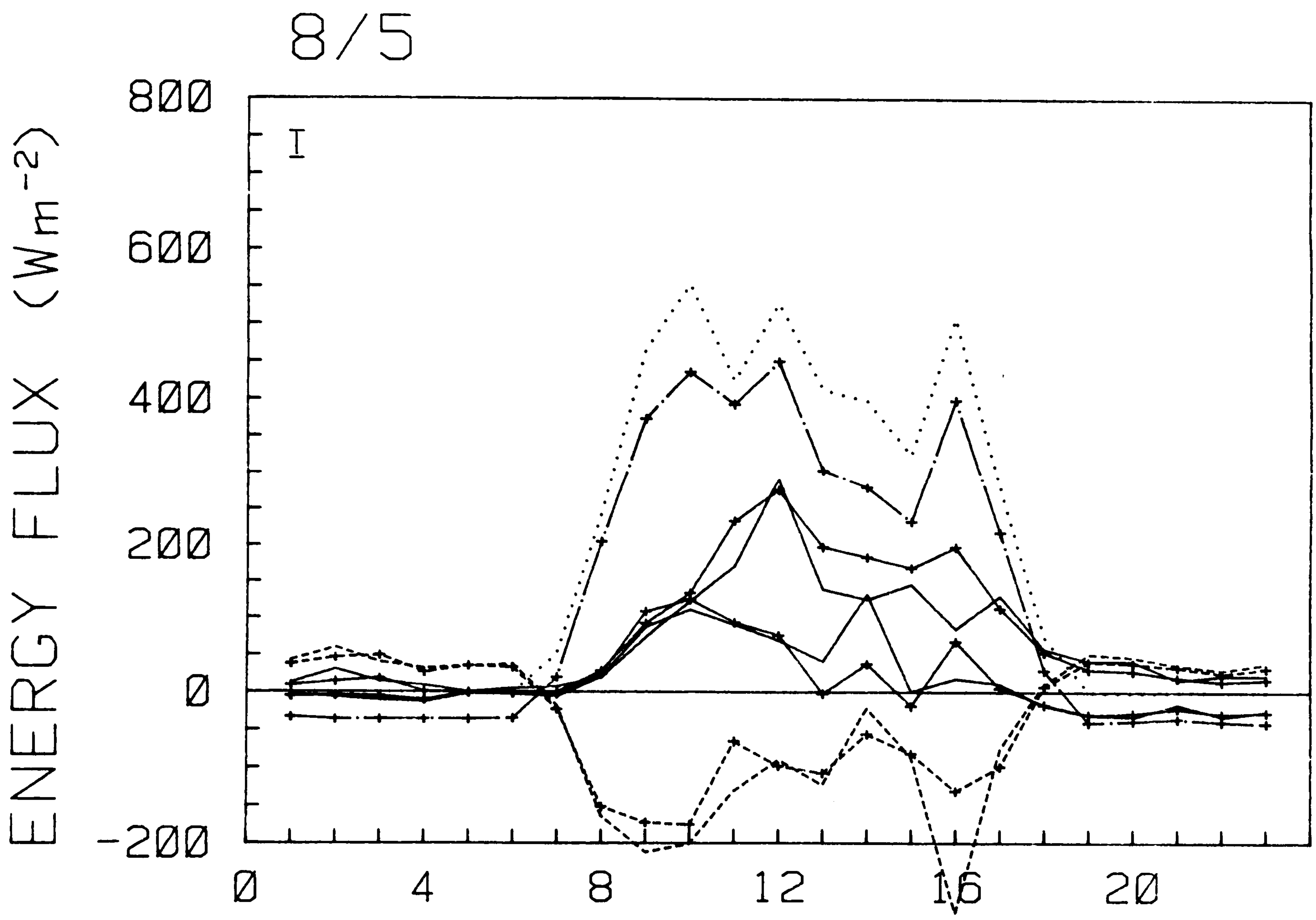

Fig. 8 I

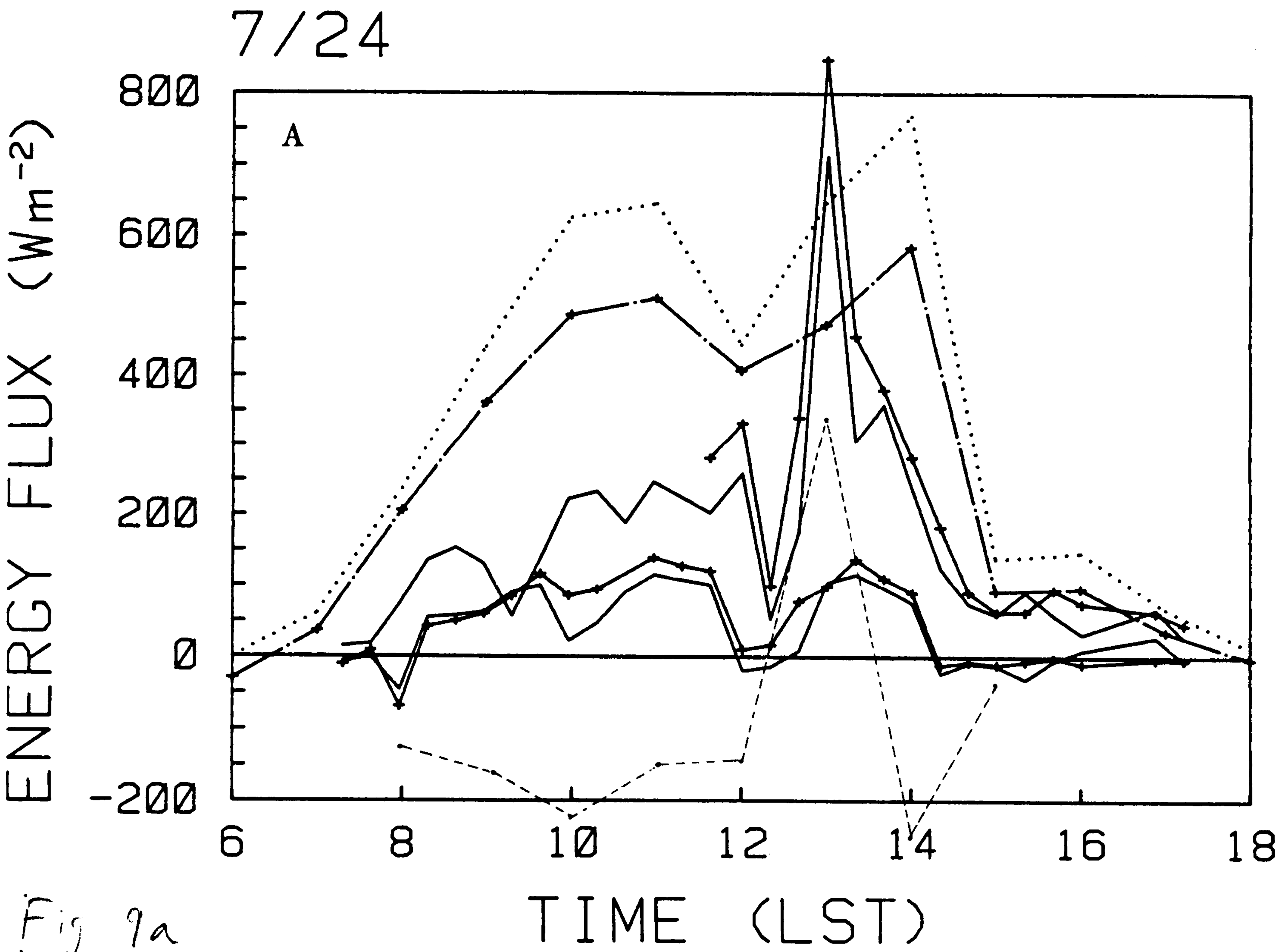

7/24
A
800
600
400
200
0
-200
ENERGY FLUX (Wm-2)
6
8
10
12
14
16
18
TIME (LST)

Fig 9a

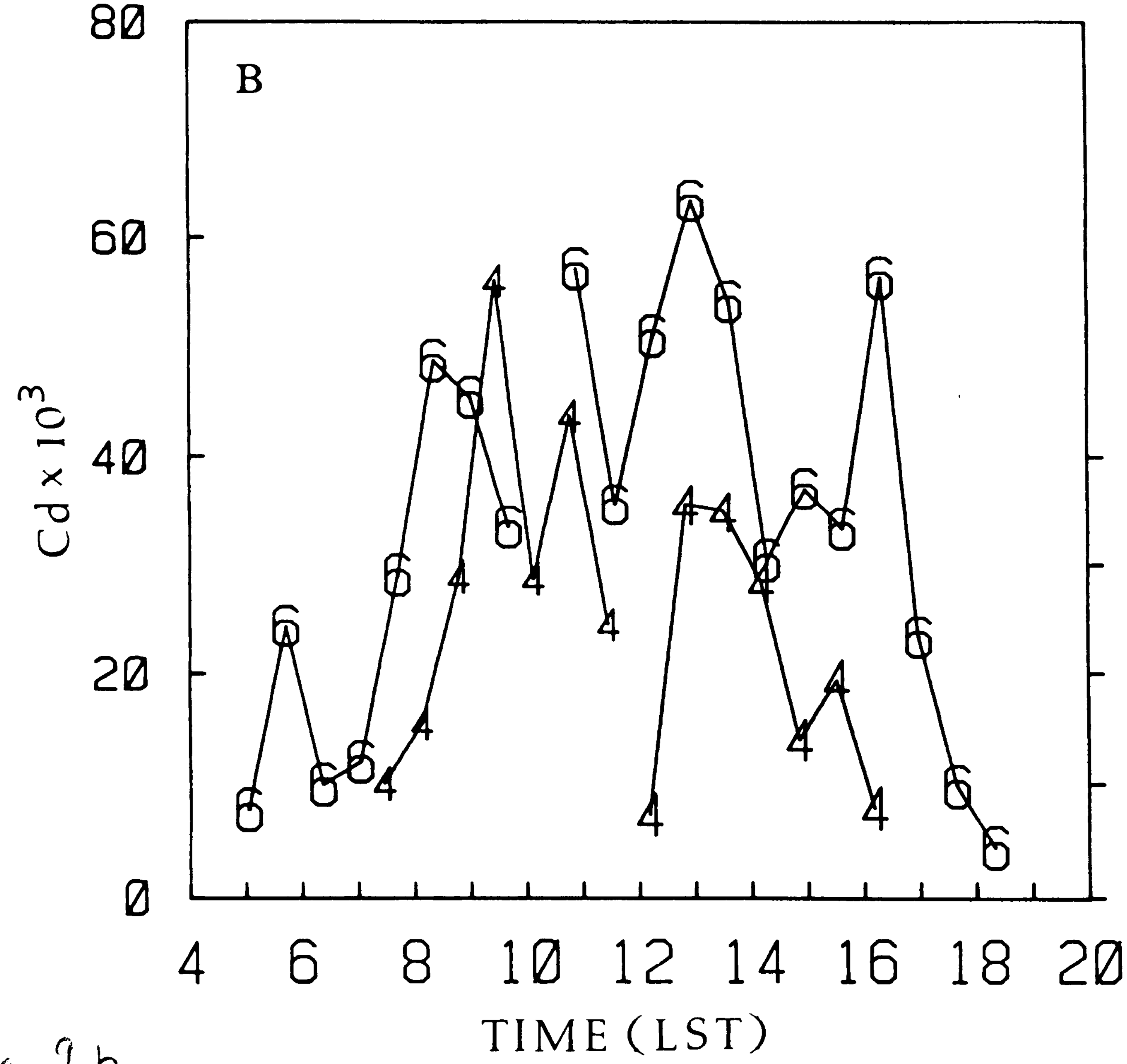

Fig 9b

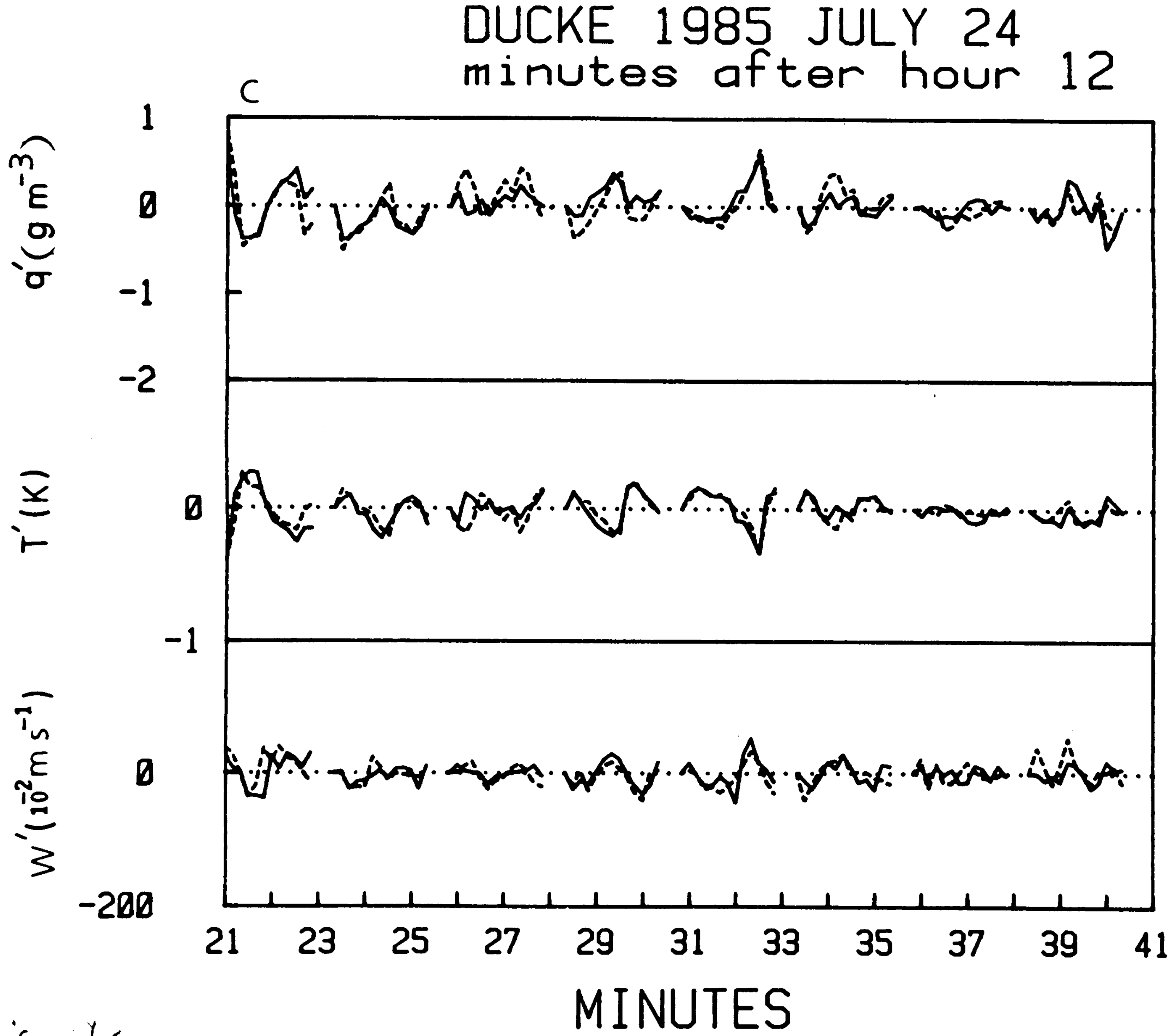

DUCKE 1985 JULY 24
minutes after hour 12
C
q'(g m^-3)
T'(K)
W'(10^-2 m s^-1)
1
0
-1
-2
0
-1
0
-200
21
23
25
27
29
31
33
35
37
39
41
MINUTES

Fig 1c

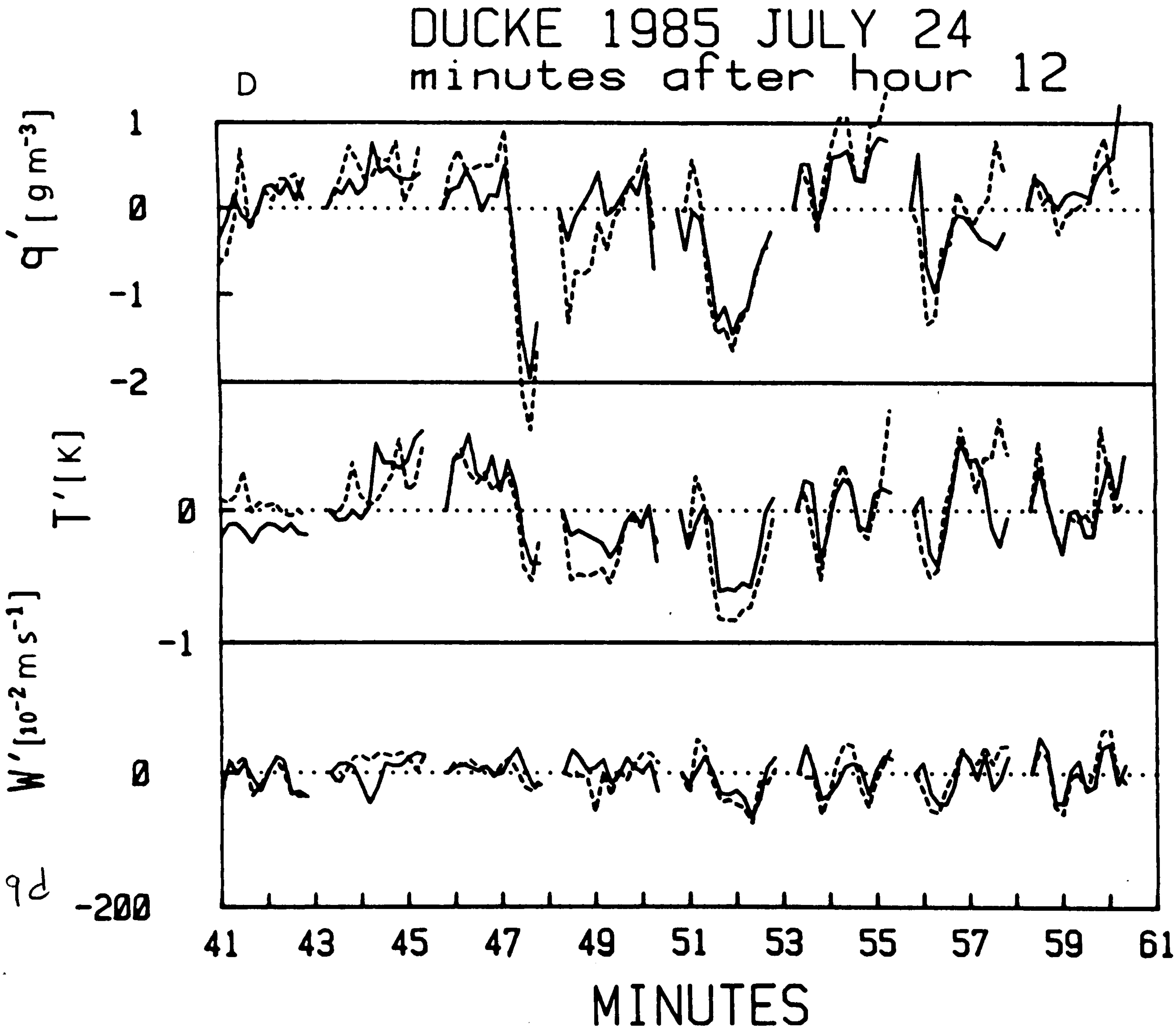
DUCKE 1985 JULY 24
minutes after hour 12
D
q' [g m^-3]
1
0
-1
-2
T' [K]
0
-1
W' [10^-2 m s^-1]
0
-200
41
43
45
47
49
51
53
55
57
59
61
MINUTES

Fig 9d

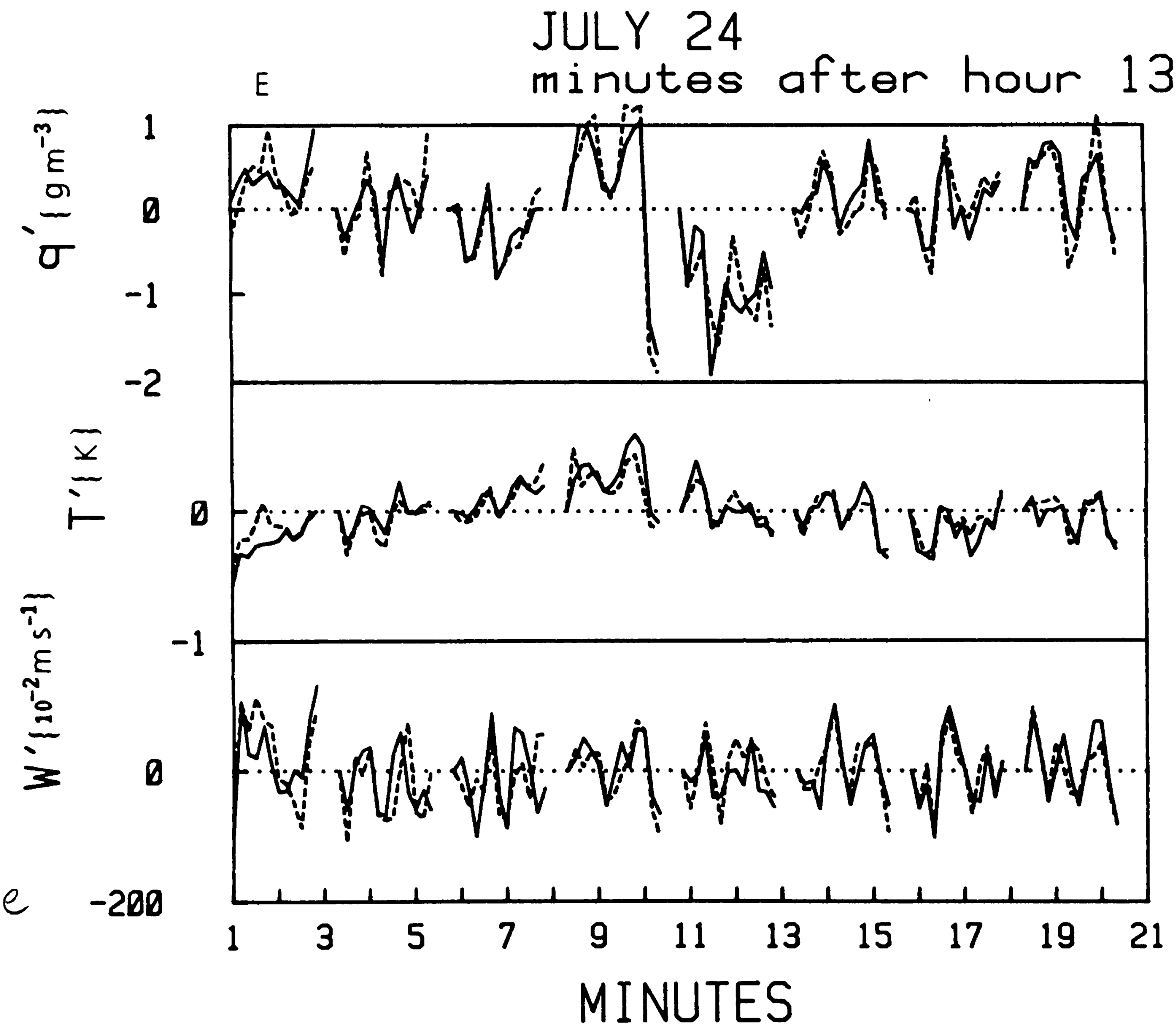
JULY 24
minutes after hour 13
E
q' {gm^-3}
1
0
-1
-2
T' {K}
0
-1
W' {10^-2 m s^-1}
0
-200
1
3
5
7
9
11
13
15
17
19
21
MINUTES

Fig 9e

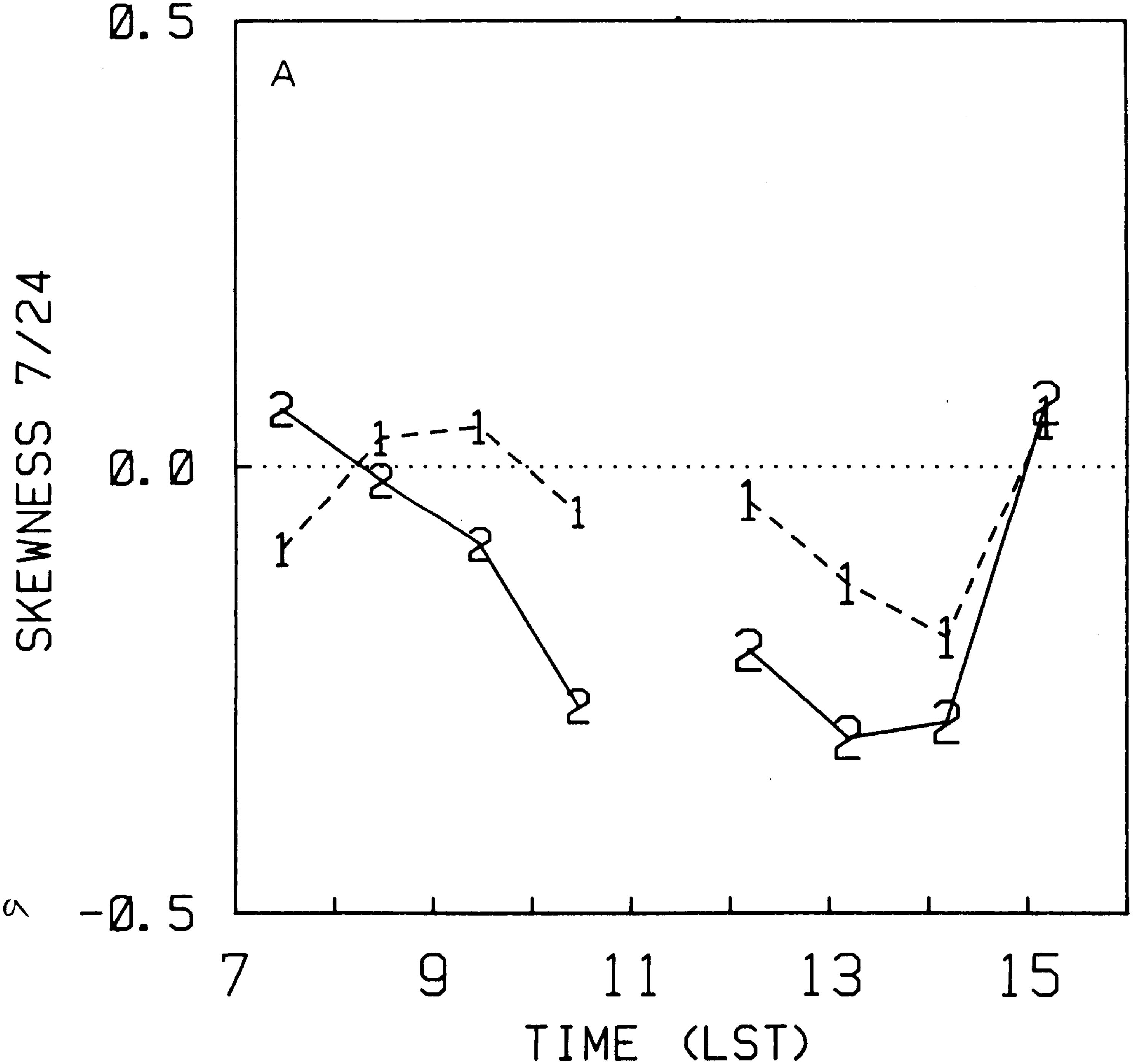

Figure 10a

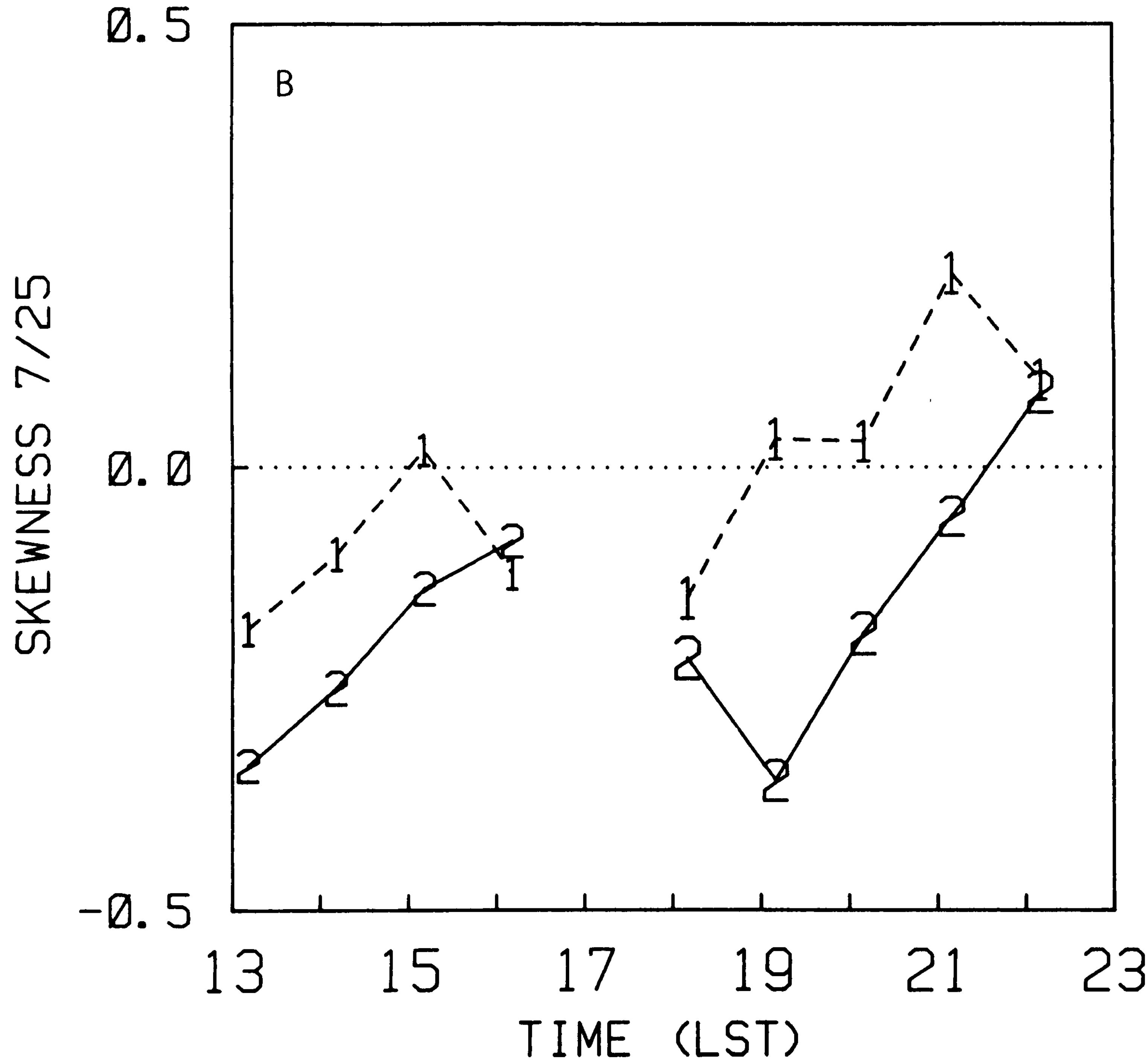

Fig. 10b

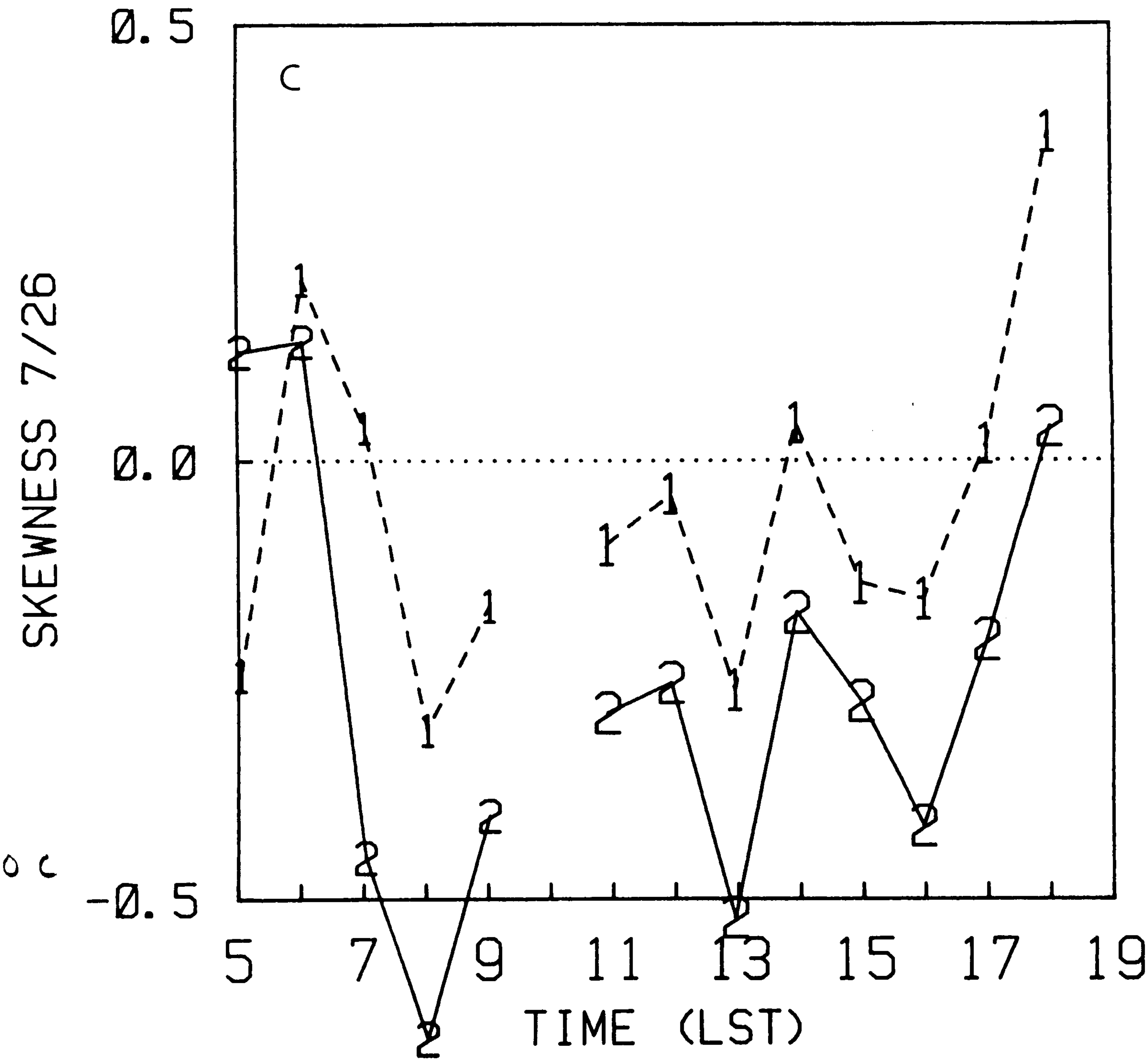

Figure 10c

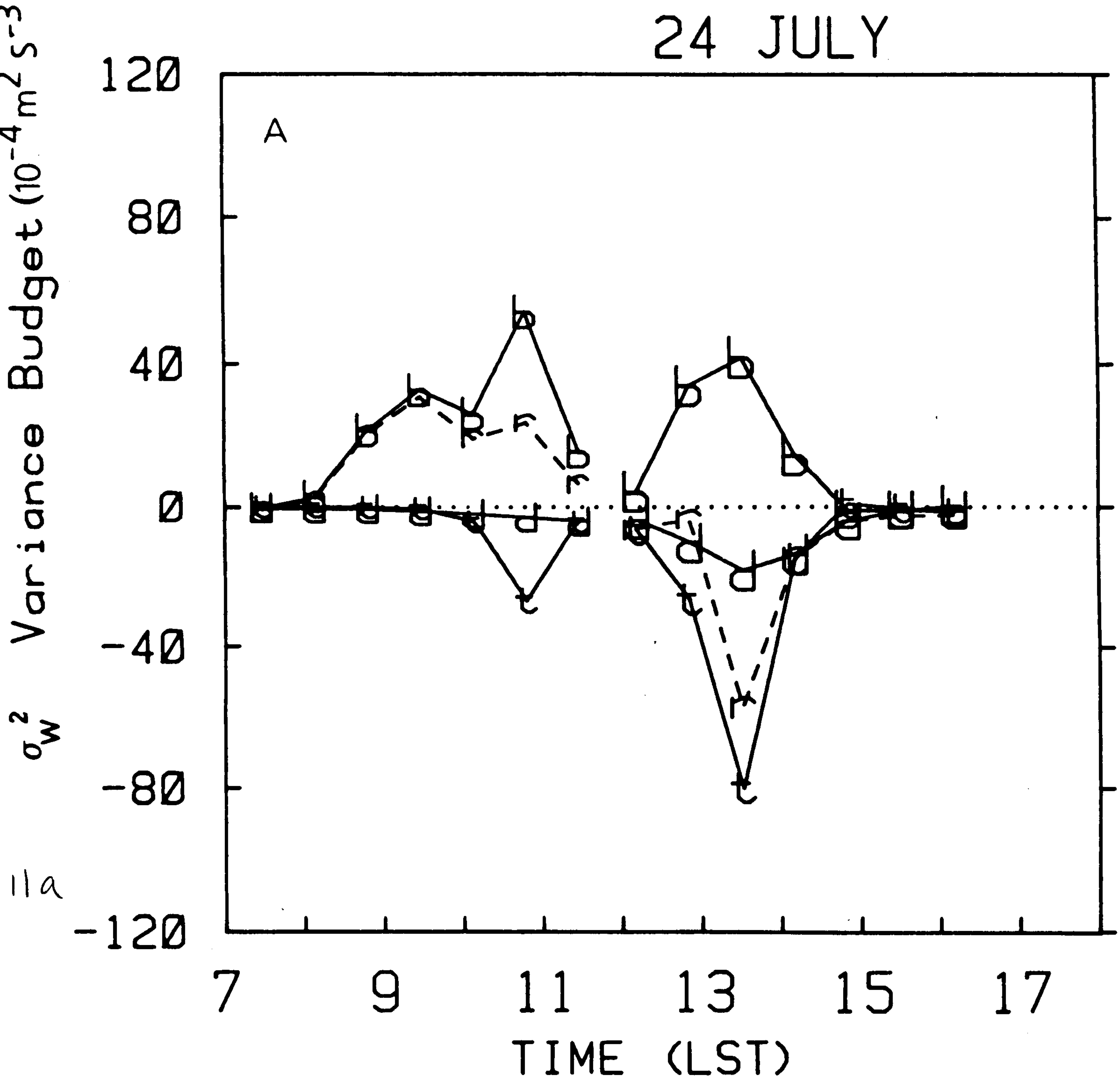
24 JULY
A
120
80
40
0
-40
-80
-120
σ_w^2 Variance Budget ($10^{-4} m^2 s^{-3}$)
7
9
11
13
15
17
TIME (LST)

Figure 11a

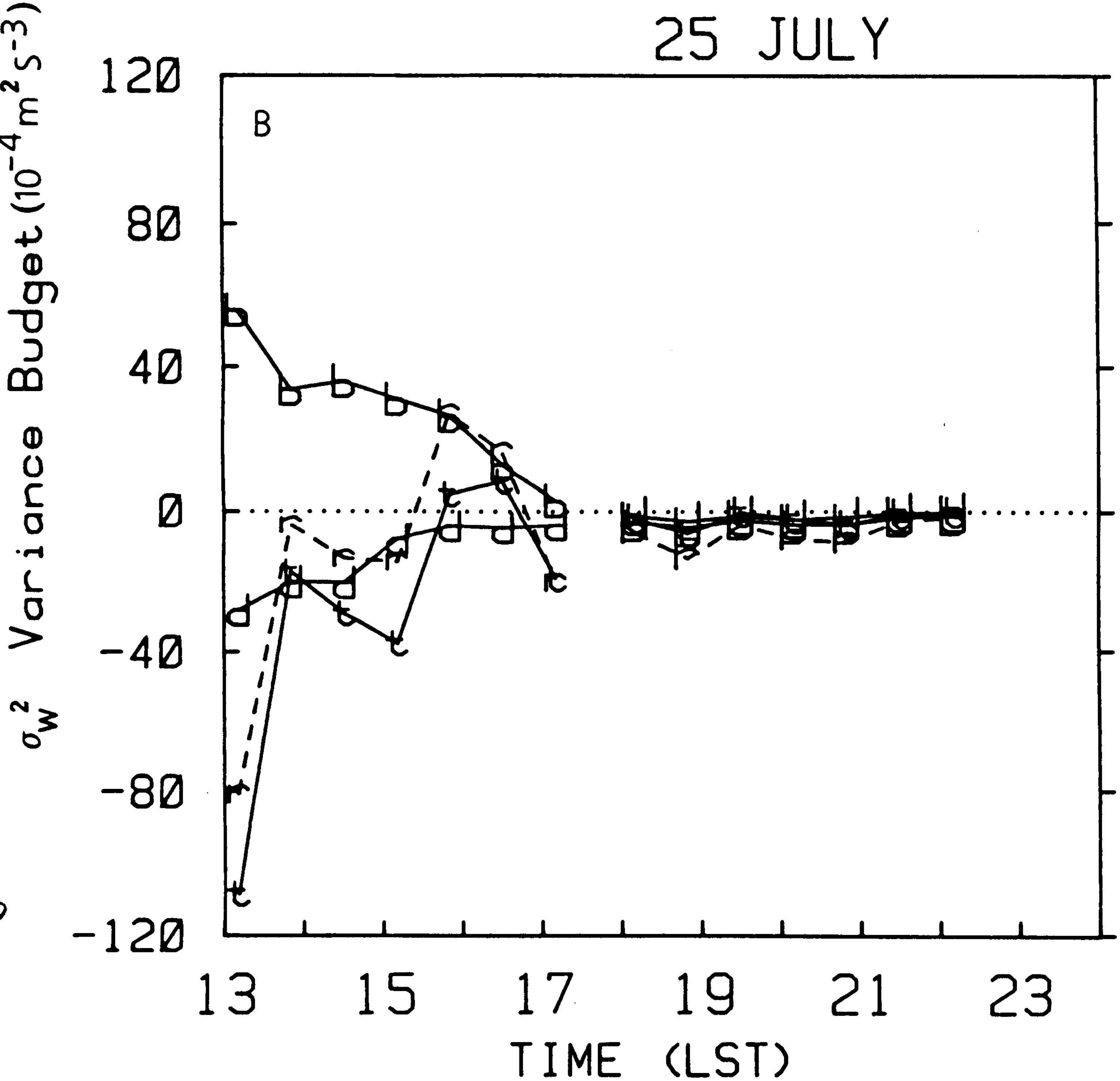
25 JULY
B
σ_w^2 Variance Budget ($10^{-4}m^2s^{-3}$)
120
80
40
0
-40
-80
-120
13
15
17
19
21
23
TIME (LST)

Fig 11b

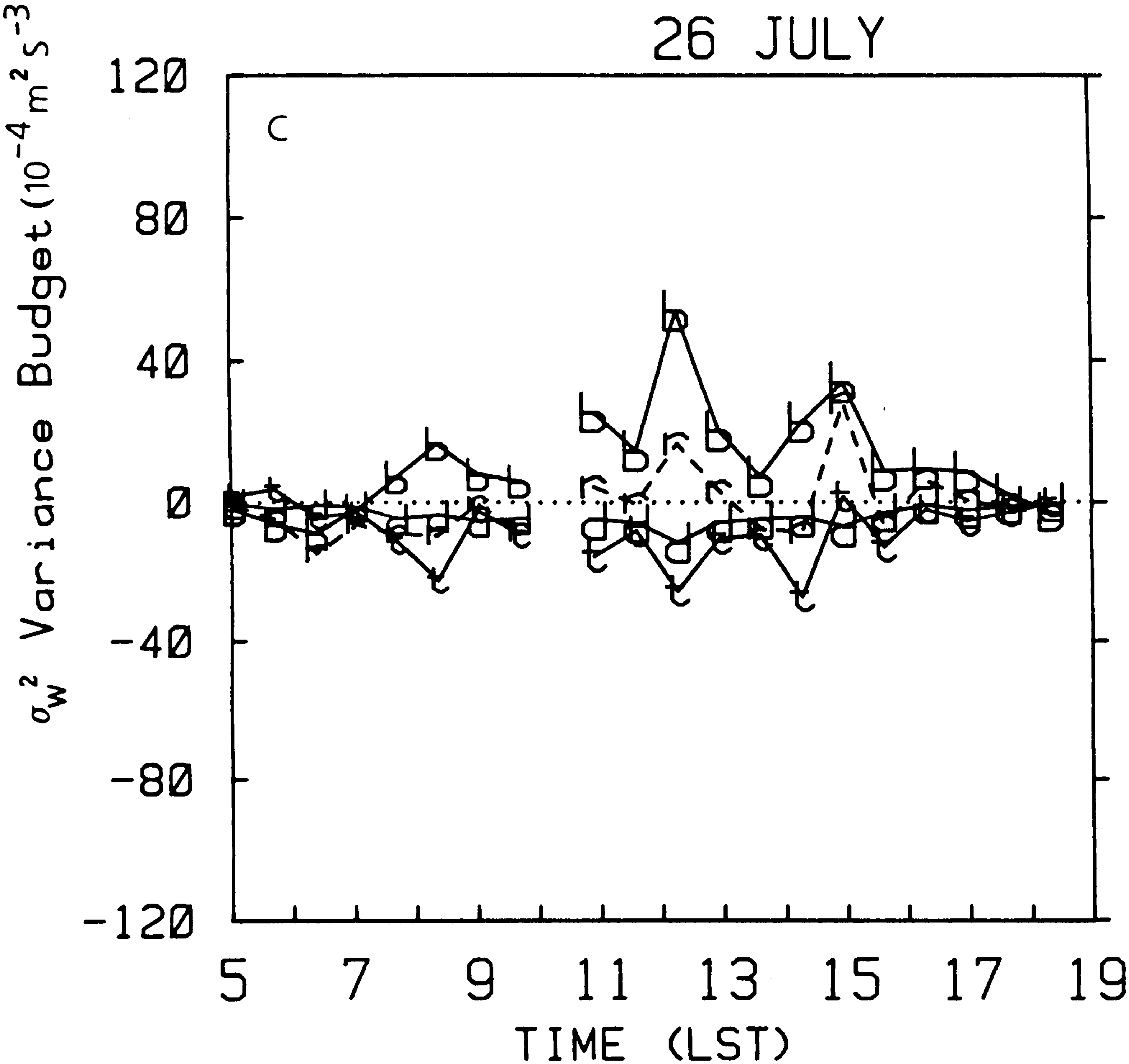
26 JULY
c
120
80
40
0
-40
-80
-120
σ_w^2 Variance Budget ($10^{-4} m^2 s^{-3}$)
5
7
9
11
13
15
17
19
TIME (LST)

Fig 11 c

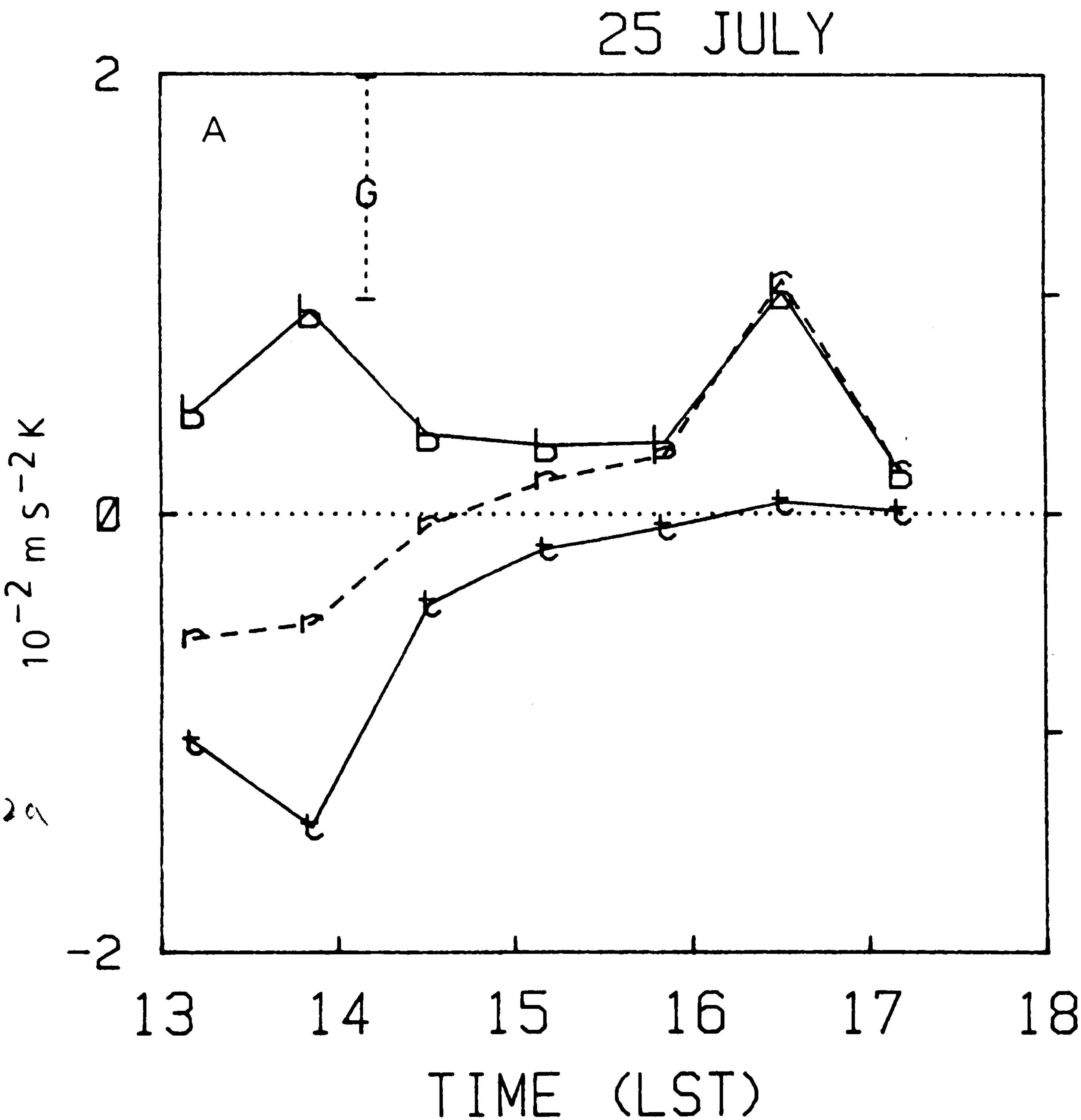

Figure 12a

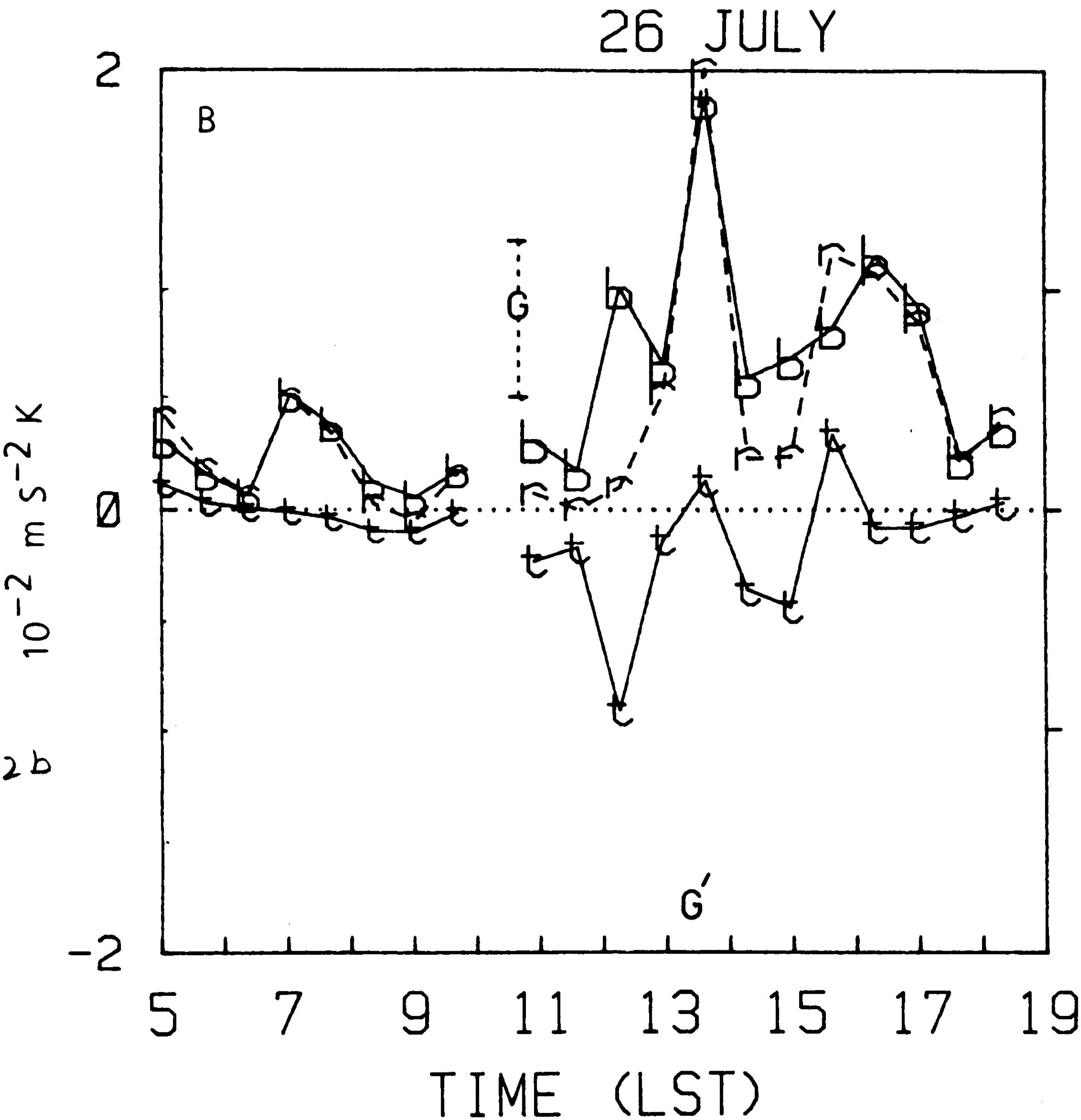

Figure 12b

APPENDIX B

Turbulent Transport

Above the

Amazon Forest

Abstract of

a thesis presented to the Faculty

of the State University of New York

at Albany

in partial fulfillment of the requirements

for the degree of

Master of Science

College of Science and Mathematics

Department of Atmosheric Science

Brian L. Stormwind

1987

Abstract

Measurements of turbulent heat, moisture, and momentum transport in a ten meter layer above the Amazon forest canopy have been made in July and August of 1985. The main objective of this thesis is obtain a better understanding of the forest-atmosphere interaction by gaining knowledge of the transport processes and the relevant scales of turbulence. Turbulent scales estimated using calculated dissipation rates and a surface layer similarity hypothesis are on the order of 100 m during convective conditions and approximately 20 m during stable periods. Detailed forest energy budgets are computed along with variance and flux budgets. This includes time series of the production, transport, and dissipation terms in the turbulence budgets of vertical velocity variance, sensible heat flux, and latent heat flux. Observations following rainfall shows disruption of the diurnal heat budget. Drastic reduction of the heat and moisture fluxes are experienced immediately after the rainfall, followed by a large latent heat flux. Passing showers create "wet, slick spots" along which convergence, and hence convection, may occur.